

Developmental Stage Specificity and the Role of Mitochondrial Metabolism in the Response of Arabidopsis Leaves to Prolonged Mild Osmotic Stress^{1[C][W][OA]}

Aleksandra Skirycz, Stefanie De Bodt, Toshihiro Obata, Inge De Clercq, Hannes Claeys, Riet De Rycke, Megan Andriankaja, Olivier Van Aken², Frank Van Breusegem, Alisdair R. Fernie, and Dirk Inzé*

Department of Plant Biotechnology and Genetics, Ghent University, B-9052 Ghent, Belgium (A.S., S.D.B., I.D.C., H.C., R.D.R., M.A., O.V.A., F.V.B., D.I.); Department of Plant Systems Biology, Flanders Institute for Biotechnology, B-9052 Ghent, Belgium (A.S., S.D.B., I.D.C., H.C., M.A., O.V.A., F.V.B., D.I.); and Max-Planck Institute for Molecular Plant Physiology, D-14476 Potsdam-Golm, Germany (T.O., A.R.F.)

When subjected to stress, plants reprogram their growth by largely unknown mechanisms. To provide insights into this process, the growth of Arabidopsis (*Arabidopsis thaliana*) leaves that develop under mild osmotic stress was studied. Early during leaf development, cell number and size were reduced by stress, but growth was remarkably adaptable, as division and expansion rates were identical to controls within a few days of leaf initiation. To investigate the molecular basis of the observed adaptability, leaves with only proliferating, exclusively expanding, and mature cells were analyzed by transcriptomics and targeted metabolomics. The stress response measured in growing and mature leaves was largely distinct; several hundred transcripts and multiple metabolites responded exclusively in the proliferating and/or expanding leaves. Only a few genes were differentially expressed across the three stages. Data analysis showed that proliferation and expansion were regulated by common regulatory circuits, involving ethylene and gibberellins but not abscisic acid. The role of ethylene was supported by the analysis of ethylene-insensitive mutants. Exclusively in proliferating cells, stress induced genes of the so-called "mitochondrial dysfunction regulon," comprising alternative oxidase. Up-regulation for eight of these genes was confirmed with promoter: β -glucuronidase reporter lines. Furthermore, mitochondria of stress-treated dividing cells were morphologically distinct from control ones, and growth of plants overexpressing the alternative oxidase gene was more tolerant to osmotic and drought stresses. Taken together, our data underline the value of analyzing stress responses in development and demonstrate the importance of mitochondrial respiration for sustaining cell proliferation under osmotic stress conditions.

¹ This work was supported by Ghent University (Bijzonder Onderzoeksfonds Methusalem project grant no. BOF08/01M00408 and Geconcerteerde Onderzoeksacties grant no. 12051403), by the Interuniversity Attraction Poles Program (grant no. VI/33), initiated by the Belgian State Science Policy Office, by the Institute for the Promotion of Innovation by Science and Technology in Flanders (predoctoral fellowships to I.D.C. and O.V.A.), and by the Research Foundation-Flanders (postdoctoral fellowship to S.D.B.).

² Present address: Australian Research Council Centre of Excellence in Plant Energy Biology, University of Western Australia, Crawley, Western Australia 6009, Australia.

* Corresponding author; e-mail dirk.inze@psb.vib-ugent.be.

The author responsible for distribution of materials integral to the findings presented in this article in accordance with the policy described in the Instructions for Authors (www.plantphysiol.org) is: Dirk Inzé (dirk.inze@psb.vib-ugent.be).

^[C] Some figures in this article are displayed in color online but in black and white in the print edition.

^[W] The online version of this article contains Web-only data.

^[OA] Open Access articles can be viewed online without a subscription.

www.plantphysiol.org/cgi/doi/10.1104/pp.109.148965

Drought stress causes reduced plant growth and, consequently, often dramatic decreases in crop yield (Boyer, 1982). With the rapidly growing world population, environmental deterioration, and the increasing need for bioenergy crops, sufficient food has to be produced on less arable land while fresh water resources become more restricted. Therefore, sustainable and equitable global food, feed, and bioenergy security relies on the development of high-yielding crop plants that can resist adverse environmental conditions. For these reasons, understanding the mechanisms underlying plant adaptation to stress is not only of primary scientific, but also of socioeconomic, importance.

Plants have evolved numerous adaptation responses to minimize the harmful effects of drought stress, summarized in the avoidance/tolerance model (for review, see Verslues et al., 2006). To avoid dehydration, mechanisms that help to balance water uptake and loss, such as stomatal closure and accumulation of compatible solutes (e.g. Pro and raffinose), are activated. These changes consequently result in reduced

transpiration and a lower water potential, respectively. Additionally, tolerance mechanisms are triggered to protect cells against damage; for instance, protective proteins are synthesized, such as dehydrins and late-embryogenesis abundant (LEA) proteins, to restrict damage to other proteins and cellular membranes, while production of antioxidants reduces the levels of harmful reactive oxygen species (ROS). Long-term water stress can be accompanied by changes, such as cuticle thickening, changing root architecture, or the hardening of cell walls. Until now, most of these drought responses have been studied only in mature tissues and under rather extreme stress conditions. In contrast, drought-associated growth restriction has received little interest, initially being considered as a secondary effect of stress related to the reduced photosynthetic activity and stomatal closure. However, after the onset of stress, growth rates have been shown to decrease rapidly, independently of photosynthesis (referred to as “short-term adjustment”), followed by growth recovery and adaptation to the new condition (referred to as “long-term adaptation”; Burssens et al., 2000; Veselov et al., 2002; West et al., 2004; Fricke et al., 2006). Therefore, although it is now accepted that plants actively reduce their growth as part of the stress response, the underlying mechanisms are still only poorly understood. These growth changes allow plants to save and redistribute resources that can become limited; for example, smaller leaves lose less water due to a reduced transpiration area, while differential growth recovery leads to beneficially higher root-to-shoot ratios (Hsiao and Xu, 2000).

In *Arabidopsis thaliana*, leaf primordia emerge as rod-like structures (20–40 μm in size) on the flank of the vegetative shoot apical meristem (SAM). Abaxial and adaxial domains become specified in this primordium and begin to form the flat lamina via lateral and distal cell proliferation. Final leaf shape is achieved during the following developmental phase, in which organ growth and histogenesis are typified by extensive cell expansion. The cell expansion phase is initiated at the distal tip, proceeds gradually in a distal-proximal manner (Donnelly et al., 1999), and coincides with the onset of postmitotic endoreduplication and the sink-to-source transition. By targeting the right age, one can harvest leaves that are entirely proliferating, expanding, or mature (Beemster et al., 2005).

The main aim of this study was to provide insight into how both proliferating and expanding leaves of *Arabidopsis* adapt to prolonged mild osmotic stress when compared with mature leaves. Therefore, a relatively mild stress assay was developed, and only leaves with proliferating, expanding, or mature cells were microdissected before expression and metabolite profiling. This experimental setup differed from published drought gene expression studies, in which mature leaves or complete plant shoots were submitted to relatively severe drought treatments with complete growth arrest or even plant death as a result

(Seki et al., 2002; Catala et al., 2007; Kilian et al., 2007; Bouchabke-Coussa et al., 2008; Giraud et al., 2008; Matsui et al., 2008; Perera et al., 2008; Weston et al., 2008; Zhang et al., 2008; Zeller et al., 2009). Stage-specific sampling together with detailed growth analysis provided candidate biological processes, genes, and metabolites that supported growth under stress-limiting conditions. These data are discussed in the context of current models of plant performance under water-limiting conditions.

RESULTS

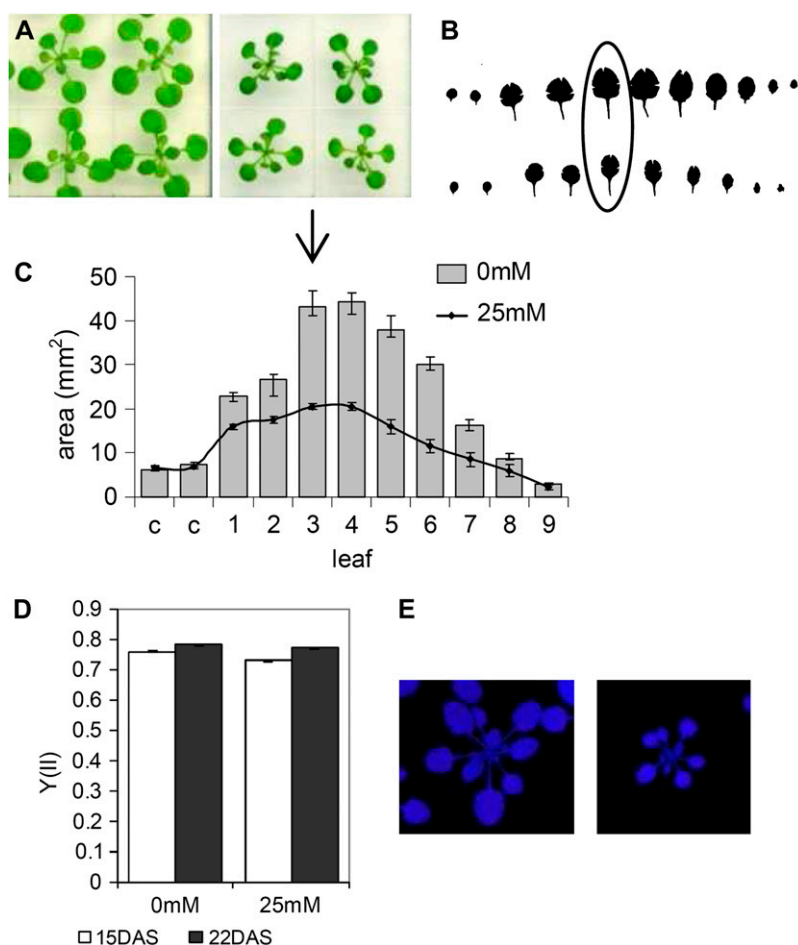
Development of a Mild Osmotic Stress Assay

To decipher the mechanisms by which water deficit affects plant growth, an experimental setup was developed that reproducibly reduced leaf size by 50% (Fig. 1, A–C). The best results were obtained with a low concentration (25 mM) of mannitol that decreases the water potential of the growth medium and, consequently, water uptake of the exposed roots. As an alternative to mannitol, the high- M_r osmoticum polyethylene glycol (PEG) 3500 was also tested; however, in this instance, the observed growth reduction was highly variable. Even when grown on the same plate, some plants developed very severe phenotypes while others appeared unaffected (Supplemental Fig. S1), complicating further analysis and data interpretation. Therefore, mannitol was used for the detailed profiling analysis and PEG was used to confirm selected results. More specifically, *Arabidopsis* seedlings were germinated and grown on medium with or without mannitol up to 22 d after stratification (DAS; Fig. 1A). In contrast to the responses reported for higher concentrations of mannitol (usually 100–300 mM), no changes in seed germination, frequency of leaf initiation (data not shown), or leaf morphology (curling and narrowing) were observed (Fig. 1, A and B). Importantly, also the operating efficiency of PSII did not change when measured with nondestructive imaging at 15 and 22 DAS, reflecting the mild character of the applied stress (Fig. 1, D and E).

Leaf Growth Adapts to the Osmotic Stress

To identify the mechanisms underlying the 50% reduction of the final leaf size when grown under osmotic stress, the third leaf that initiates and subsequently develops under stress conditions (Fig. 1C) was used for further analysis. As the final leaf size depends on the developmental window and rates of cell division and expansion (Beemster et al., 2005), these parameters were assessed by kinematic analysis (De Veylder et al., 2001). This analysis provides information on cell area, cell number, number of guard cells, and cell division and expansion rates throughout leaf development (Fig. 2). To obtain these data, leaves were harvested daily from the early meristematic stage (9 DAS and approximately 0.1 mm^2 in size) to maturity

Figure 1. Mannitol setup. A, Plants at 22 DAS grown in the absence (left) or presence (right) of 25 mM mannitol. B, Leaf series (third leaf encircled). C, Leaf area calculation. The arrow marks leaf 3 used in further analysis. D, Measurement of operating efficiency of PSII. E, Images of the effective PSII quantum yield (left, 0 mM; right, 25 mM).



(22 DAS). Leaf primordia younger than 9 DAS were too small to dissect. At 9 DAS, growth of leaf 3 was driven exclusively by cell division, as demonstrated by expression of the B-type cyclin *CYCB1;2* in the whole leaf primordia (Fig. 3B).

Cellular measurements demonstrated that both reduction in cell number and size contributed equally to the reduced area of mature leaves grown on mannitol (Fig. 2, A–C). Already at the first measurements at 9 DAS, both leaf size and cell number had significantly decreased, while cell size was not affected by the treatment (Fig. 2, A–C). Intriguingly, neither cell division rates nor the developmental cell proliferation window was reduced (Fig. 2E); on the contrary, division rates were approximately 10% higher between 12 and 16 DAS, partially compensating for the initial reduction in cell number (Fig. 2E; Supplemental Fig. S2). As the frequency of leaf initiation was also unchanged, the observed reduction in cell number had to arise very early, during the first few days after leaf initiation, thus escaping analysis. Cell differentiation was unaffected, starting from day 10 both under normal and stress conditions. Cell expansion rates were initially reduced in stressed leaves but reached control levels at day 15 and exceeded them between days 18 and 20, partially compensating the initial

reduction in cell size (Fig. 2, C and F; Supplemental Fig. S2). Leaf growth rates gradually decreased, and leaf 3 approached maturity by day 22 (Fig. 2D). As alterations in cell area can be associated with changes in endoreduplication (Inzé and De Veylder, 2006), the ploidy distribution was determined, but no significant differences were measured either in onset or in level of endoreduplication (Supplemental Fig. S3). Similar to mannitol, PEG also influenced both cell number and size, contributing to the reduced leaf area; however, the effects were predominantly on cell number, while cell size was reduced only marginally (Supplemental Fig. S4).

Cell drawings revealed further differences between control and mannitol-stressed leaves. The shape of the epidermal cells was clearly affected: cells were not only smaller but also less lobed (Fig. 2H), relating to an approximately 15% decrease in cell perimeter when calculated per cell area (Fig. 2I). Moreover, although the first stomata appeared simultaneously in both control and stressed leaves, their number had decreased when calculated per total cell numbers (stomatal index [SI]; Fig. 2G). The maximum SI reduction was calculated at 13 DAS (more than 65%), but the difference diminished to 23% at 22 DAS (Supplemental Fig. S2). In contrast to the SI, trichome density increased in mannitol-grown plants when calculated per leaf area.

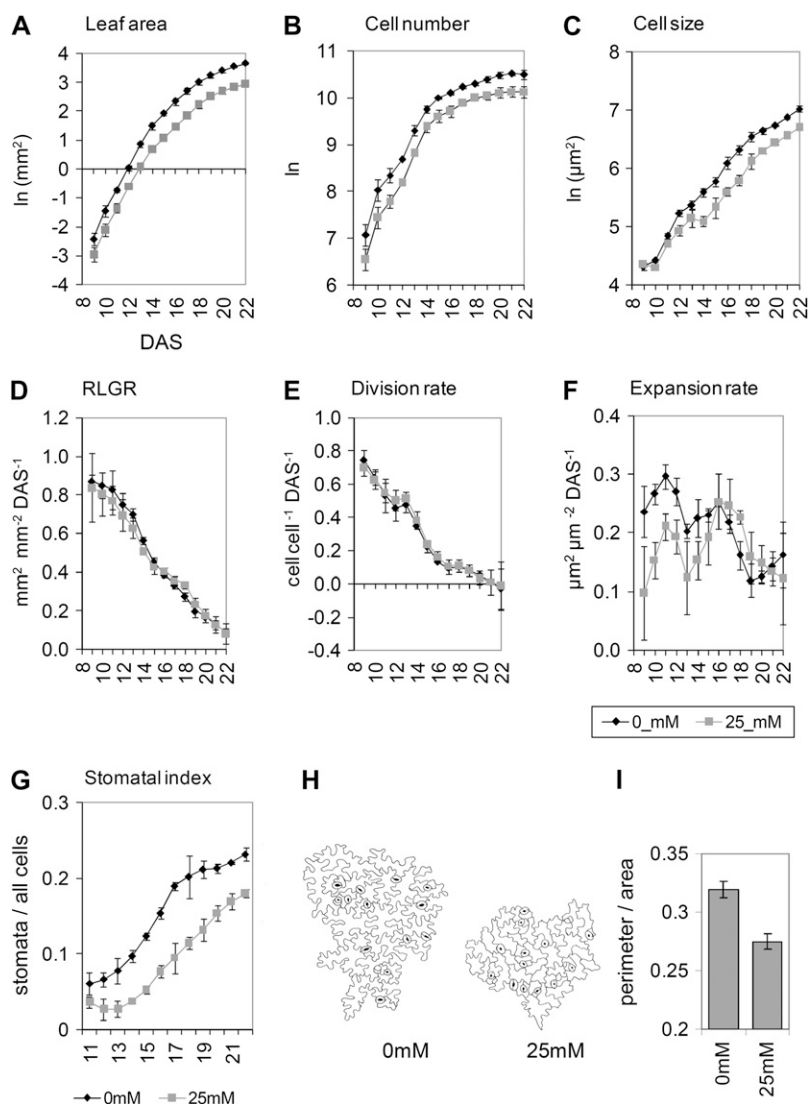


Figure 2. Kinematic analysis of leaf 3 dissected from plants grown with or without 25 mM mannitol from 9 to 22 DAS. A, Leaf area. B, Cell number. C, Cell size. D, Relative leaf growth rate (RLGR). E, Relative cell division rate. F, Relative cell expansion rate. G, St. H, Example of cell drawings of epidermal cells. I, Cell perimeter per cell area (perimeter/area) from epidermal cells. Data are means \pm SE of three independent experiments. Leaves 8 to 10 were used to measure leaf area. Cellular data are from four leaves in each experiment.

Changes in SI and trichome density could be measured for PEG-grown plants as well (Supplemental Fig. S4).

Experimental Setup

To obtain molecular insight into growth adaptation to osmotic stress, samples of exclusively proliferating leaf primordia (P) and expanding (E) and mature (M) leaves were subjected to whole-genome transcript profiling (Fig. 3A). Additionally, the aerial parts of whole seedlings at stage 1.03 (Boyes et al., 2001) were included and compared with the leaf samples. To complement the transcript data, metabolites were measured in 1.03 seedlings and E and M leaf samples. The small size of the P leaves prompted the development of a microdissection method with RNAlater (see "Materials and Methods") that made the samples unsuitable for metabolite measurements. At the time of harvest, growth rates of control and stressed plants were identical, allowing us to study growth adaptation

to drought rather than growth inhibition. Statistical analysis was used to identify significant changes with respect to developmental stage (P, E, and M ["significant leaf stage effect"]; Supplemental Table S1) and treatment (with and without 25 mM mannitol ["significant osmotic stress effect"]; Supplemental Tables S2–S5). Differential transcripts were investigated with MapMan for pathway visualization (Thimm et al., 2004) and PageMan to calculate functional overrepresentation of MapMan categories (Usadel et al., 2006; Fig. 4; Supplemental Fig. S5). Data were also compared with selected publicly available microarray experiments, mainly from AtGenExpress (see "Materials and Methods"; Supplemental Table S3).

Transcript and Metabolite Changes during Normal Leaf Development

To establish a baseline of changes associated with normal leaf development, transcripts and metabolites with significant leaf stage effects were identified

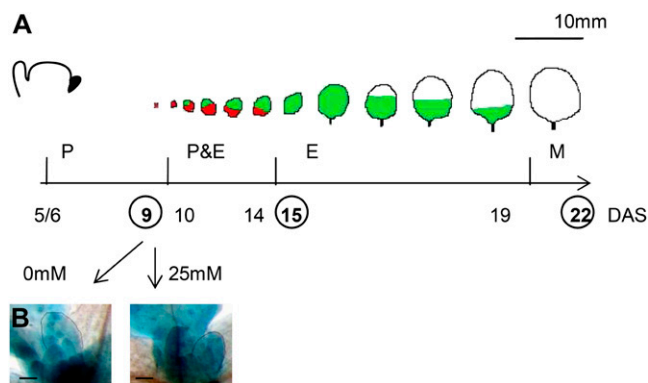


Figure 3. Experimental setup. A, Schematic representation of Arabidopsis leaf development. P cells, red; E cells, green; and M cells, white. The scale bar only applies to the leaves, not to the representation of the SAM. Leaf 3 initiates at approximately 5 DAS; all cells proliferate at 9 DAS, expand exclusively around 15 DAS, and approach maturity at 22 DAS, both under control and stress conditions. Samples for profiling analysis were dissected at 9, 15, and 22 DAS. B, GUS activity staining of leaf 3 from *CYCB1;2-GUS* plants at 9 DAS grown without or with 25 mM mannitol. The expression of *CYCB1;2* is closely related to cell division activity.

(0–0 mM), providing details on proliferating-to-expanding (P/E) and expanding-to-mature (E/M) stage transitions. In total, 2,800 transcripts could be assigned to eight expression clusters with 2-fold expression and global test (<0.05) cutoffs between any of the two stages, and the abundance of 12 metabolites varied between E and M leaves (Supplemental Fig. S5; Supplemental Tables S1 and S4). As expected, the transcriptome of P leaves (group 1 in Supplemental Fig. S5) was enriched for categories linked to mitotic cell cycle and cell division; E leaves were characterized by high expression of cell wall-related genes (group 2), while senescence markers (e.g. *SEN1* and *NAC92*) appeared exclusively in M leaves. The expression of genes associated with the mitotic cell cycle, such as B-type cyclins and kinesins, was reduced sharply at the P/E transition (group 1), whereas transcripts related to DNA and protein synthesis decreased gradually across the three developmental stages (group 7). Transcripts related to photosynthesis, primary and secondary metabolism, light signaling, transport, and auxin and redox regulation increased at the P/E transition and remained high in M leaves (group 4). Exit from expansion into maturity resulted in further changes: on the one hand, transcripts associated with cell wall and fatty acid metabolism (group 6), a number of amino acids (e.g. Gln and Asn), and organic acids (such as citric acid) decreased; on the other hand, abiotic stress-related pathways, such as genes encoding enzymes from raffinose metabolism, peaked in the M leaves (Supplemental Fig. S5). In summary, these data demonstrate extensive differences, consistent with known processes, between the three developmental stages, confirming the growth analysis and verifying the sample selection and harvesting protocols.

Adaptation to Osmotic Stress Depends on the Leaf Developmental Stage

Mild osmotic stress (25 mM mannitol) resulted in alterations in the levels of several hundred transcripts. In total, 399, 741, and 614 transcripts were up-regulated and 97, 632, and 374 transcripts were down-regulated in P, E, and M leaves, respectively (Fig. 4A; Supplemental Table S2). Based on the Venn diagram, we delineated lists of genes with altered expression levels due to osmotic stress in one or more developmental stages, revealing hundreds of transcripts affected by mannitol exclusively in one leaf stage and only very few genes that were differentially expressed across the three stages. Overall, the stress response in P and E leaves was more similar, while in fully grown M leaves it was most distinct, especially when compared with P leaves (Fig. 4B). Similarly, metabolite analysis of E and M leaves revealed distinct metabolite profiles (Fig. 5; Supplemental Table S4). Expression of 24 genes that were differentially up- or down-regulated by osmotic stress in one or more of the leaf stages and belonged to different functional categories was checked with quantitative reverse transcription (qRT)-PCR (Supplemental Fig. S6). The majority of the changes could be validated in independent mannitol and PEG experiments.

Seedling Samples Are Most Similar to the E Leaves

To learn how many stress-regulated genes and metabolites would have been detected with whole seedlings, osmotic stress effects on transcriptome and metabolome of three leaf stages were compared with seedling shoots at stage 1.03. For the seedling, 244 up-regulated and 59 down-regulated genes and four up-regulated and 12 down-regulated metabolites were detected, altogether considerably fewer than for any of the leaf developmental stages (Supplemental Table S2). Overall, the changes were most consistent with those of growing and particularly E leaves; more than 80% of the changes were also measured in the E samples (Supplemental Fig. S7). Importantly, almost none of the transcripts that changed exclusively in the P or M stage were found in the seedling samples. In summary, utilizing whole shoots substantially diluted information and stressed the value of sampling leaves at different developmental stages.

M Leaves Are Characterized by Classical Drought Response While Biotic Stress Genes Are Up-Regulated in the Growing Leaves

In addition to the dissection of responsive genes through the overrepresentation analysis of MapMan functional categories, we investigated whether these genes were affected in other microarray experiments (see “Materials and Methods”). Comparison with the publicly available stress expression data revealed significant overlap, irrespective of the leaf stage (Supplemental Table S3). However, only M and, to a lesser extent, E leaves showed the classical water stress response as determined in previous whole-plant stud-

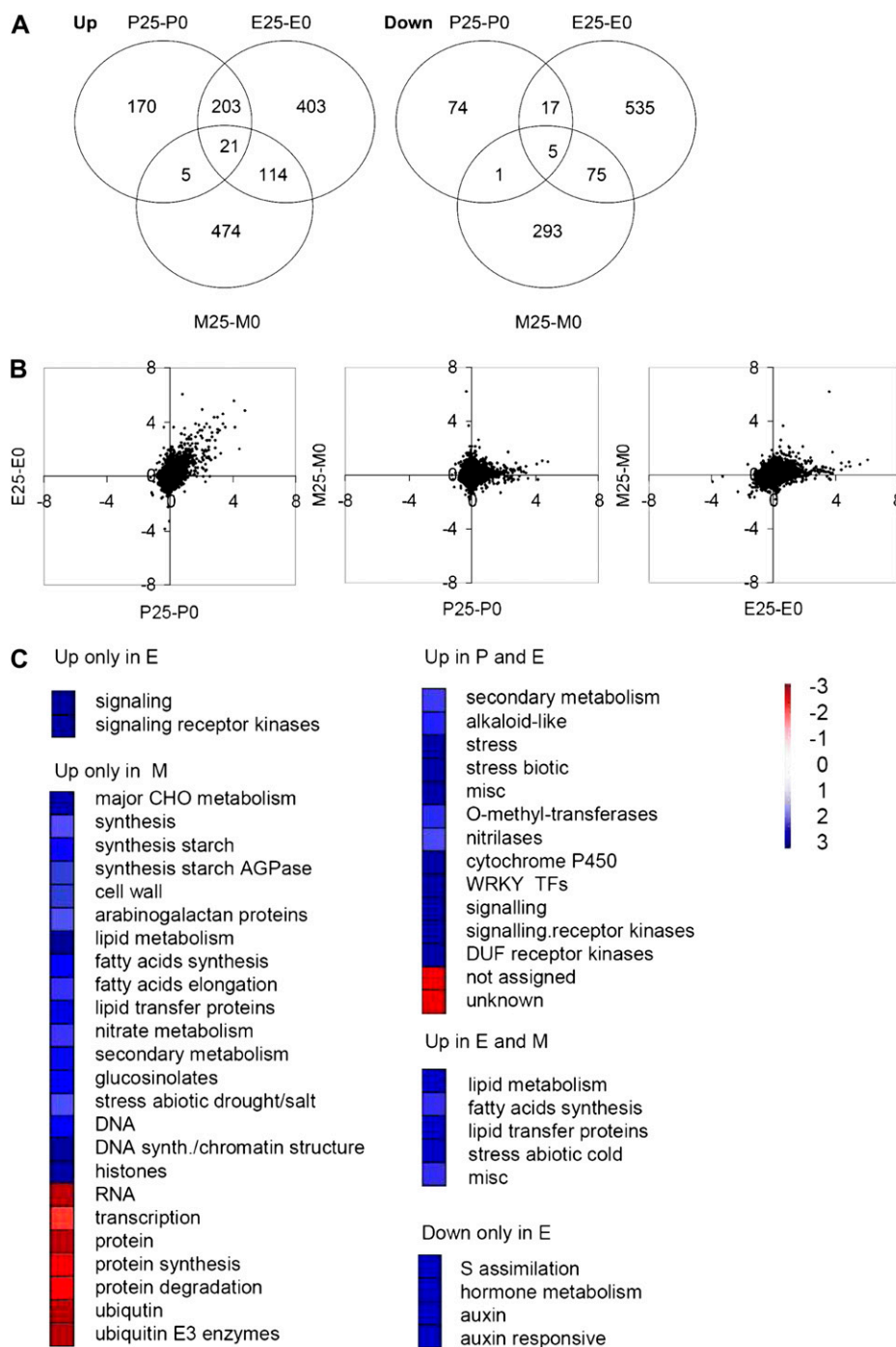
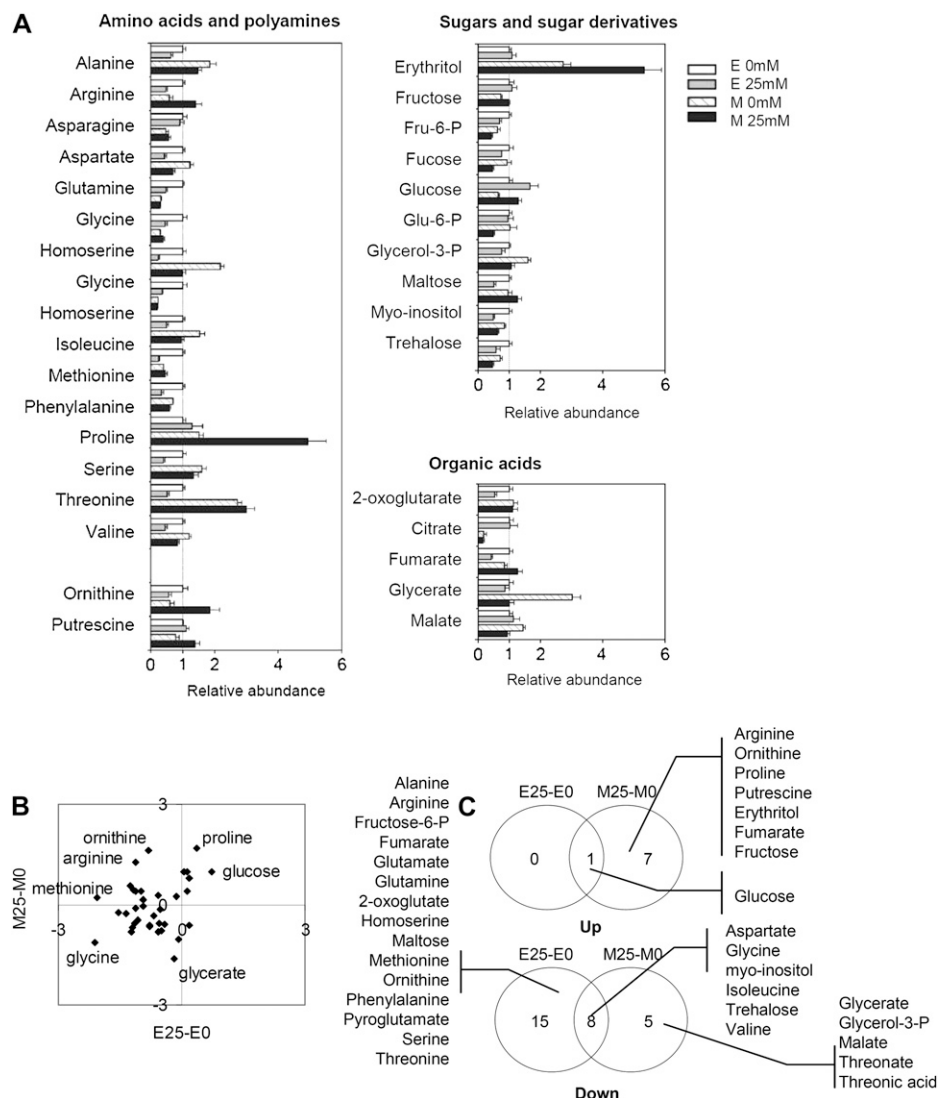


Figure 4. Functional analysis of transcripts that are significantly affected by osmotic stress. A, Venn diagram grouping of genes differentially regulated by osmotic stress in P, E, and M leaves (global test; $P < 0.05$). B, Log_2 fold changes (25–0 mM) for all analyzed genes (>20,000) used to construct scatter plots. Note the similarity between responses of P and E leaves and almost no overlap between P and M stages. C, Functional analysis with MapMan categories and the PageMan overrepresentation tool. Significantly enriched or depleted functional groups are represented in blue or red, respectively. CHO, Carbohydrate; DUF, domain of unknown function.

ies. Expression of abiotic stress markers (e.g. *RD29B*, *RD29A*, *RD22*, and *ATHVA22E*), *LEA* genes (e.g. *COR15* and *ERD10*), and genes involved in fatty acid biosynthesis (e.g. *CER1* and *KCS1*) and lipid transfer, important for cuticle thickening, was induced (Fig. 4C; Table I; Supplemental Tables S2 and S3). The role of abscisic acid (ABA) during abiotic stress is well documented, and comparison with ABA addition data revealed a significant overlap for both E and M leaves (Supplemental Table S3), and expression of

genes encoding the ABA biosynthetic enzymes, *AAO1* and *AAO2*, was also induced (Table I). Pro, a typical drought-induced metabolite, its precursor Gln, and other metabolites classically associated with drought stress, erythritol and putrescine, accumulated exclusively in M leaves (Supplemental Fig. S5; Supplemental Table S4). Moreover, induced expression of *CHS*, *FLS*, and *PAP1* genes suggested a possible accumulation of flavonol compounds, again specifically in the M leaves (Table I; Supplemental Table S2).

Figure 5. Distinct metabolite profiles of E and M leaves subjected to osmotic stress are distinct. A, Relative abundance of all the measured metabolites. B, Log₂ fold changes (25–0 mM) for all analyzed metabolites used to construct a scatter plot. C, Venn diagram with metabolites listed.



In contrast to M leaves, both P and E leaves were enriched for genes classically associated with biotic stress, and comparison with available microarrays of wounded plants or plants treated with pathogens, flagellins, oxidative stress, ethylene, and salicylic acid revealed a significant overlap (Fig. 5; Table I; Supplemental Tables S2 and S3). This overlap consisted of WRKY transcription factors (e.g. WRKY30 and WRKY33), methyltransferases, cytochrome P450 enzymes, pathogen-related proteins (chitinases, PR4, and PR5), mildew resistance locus proteins (MLO3, MLO6, and MLO12), disease resistance proteins, mitogen-activated protein kinases (MPK2 and MPK3), and indole glucosinolates/camalexin biosynthesis proteins (MYB51 transcription factor, CYP79B2, CYP83B1, CYP81F2, CYP71A13, and CYP71B15).

Osmotic Stress Affects Sugar and Amino Acid Contents

Sugars and amino acids are expected to play a major role in plant adaptation to stress (for review, see Seki

et al., 2007). A comparison of the stress response of E and M leaves with publicly available Glc addition and carbon starvation experiments revealed a significant enrichment of sugar-responsive genes (Supplemental Table S3). This increase in Glc predicted from the transcript data could be experimentally confirmed by metabolite profiling (Fig. 5). Similar to Glc, starch also accumulated in E and M leaves, as shown by Lugol’s staining (Fig. 6). Furthermore, genes encoding enzymes involved in starch synthesis (such as starch-branching enzyme 2) and the ADP-Glc pyrophosphorylases (APL2, APL3, and APL4) were up-regulated only in M leaves, while those encoding starch-degrading enzymes (e.g. the β-amylases BMY-3, BMY-5, and BMY-8) were down-regulated in both E and M leaves (Fig. 6; Supplemental Table S2). In contrast to sugars, levels of nine out of 16 measured amino acids were reduced in E, but not in M, leaves (Fig. 5). Summarizing, prolonged osmotic stress caused accumulation of soluble sugars and starch in E and M leaves, whereas the amino acid content was reduced in the E tissues.

Table 1. List of selected key genes involved in the biological processes affected by osmotic stress

Expression changes are presented as log₂. Significance (global test; *P* < 0.05) is indicated in boldface. DELLA targets identified by Navarro et al. (2008) are marked with X.

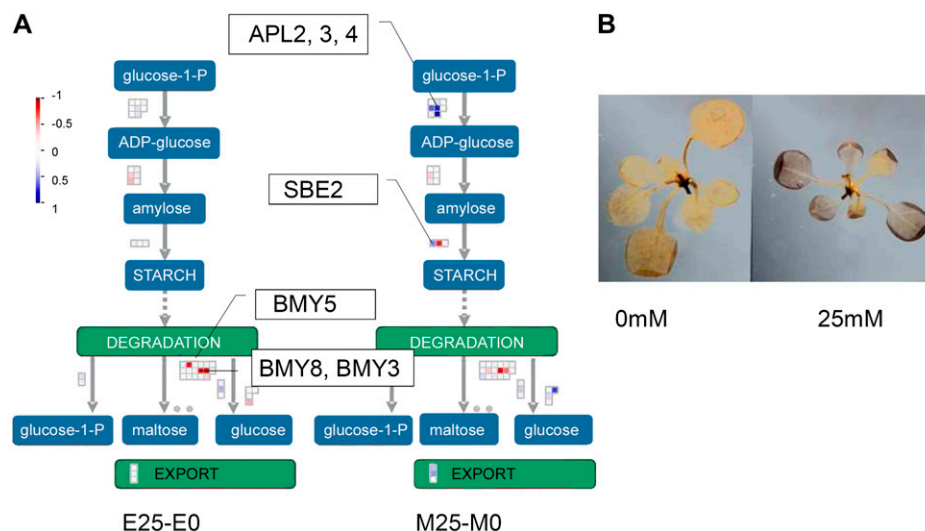
Locus	Name	Log ₂ P25-0	Log ₂ E25-0	Log ₂ M25-0	DELLA
Abiotic stress markers					
AT5G52300	RD29B	-0.19	0.31	1.61	
AT5G52310	RD29A	-0.59	1.52	1.40	
AT2G42540	COR15A	-0.13	0.88	1.12	
AT5G25610	RD22	0.71	1.38	1.09	
AT2G42530	COR15B	-0.09	1.25	1.03	
AT1G20450	ERD10	-0.22	1.25	0.99	
AT2G17840	ERD7	-0.09	0.36	0.94	
AT1G01470	LEA14	-0.24	0.59	0.83	
AT2G30870	ERD13	0.71	1.20	0.79	
AT4G19120	ERD3	-0.25	0.12	0.52	
Fatty acids/cuticle					
AT1G01120	KCS1	0.41	0.03	0.59	
AT2G38530	LTP2	0.83	6.09	1.12	
AT2G38540	LTP1	0.06	0.61	0.49	
AT1G02205	CER1	-0.07	-0.09	1.01	
AT1G68530	CUTICULAR 1	0.27	0.61	0.46	
AT1G67730	GLOSSY8	0.07	0.44	0.45	
ABA synthesis					
AT5G20960	AAO1	0.50	1.21	0.79	
AT3G43600	AAO2	0.07	0.77	0.55	
Flavonoids					
AT5G13930	CHS	-0.36	-0.02	1.16	
AT5G08640	FLS	-0.46	-0.31	0.87	
AT1G56650	PAP1 TF	-0.01	0.73	0.84	
Biotic stress markers					
AT2G39200	ATMLO12	0.93	3.08	0.40	
AT3G45290	ATMLO3	1.55	1.54	0.29	
AT1G61560	ATMLO6	0.56	0.82	0.00	
AT2G44490	PEN2	1.60	1.01	-0.04	X
AT4G01700	Chitinase	2.26	1.94	-0.11	X
AT1G33590	Disease resistance	1.30	0.93	0.51	X
AT3G45640	MPK3	0.62	0.97	0.05	X
AT1G59580	MPK2	0.42	0.47	0.26	
AT1G75040	PR-5	2.19	3.65	0.47	
AT4G23810	WRKY53	1.34	1.52	0.04	
AT2G38470	WRKY33	1.08	2.75	0.00	X
AT2G23320	WRKY15	0.76	0.59	0.17	X
Indole glucosinolates/camalexin					
AT5G57220	CYP81F2	1.82	3.80	0.04	
AT2G30770	CYP71A13	2.42	2.65	0.37	
AT4G39950	CYP79B2	1.61	2.14	0.91	
AT2G22330	CYP79B3	0.19	1.28	0.84	
AT4G31500	CYP83B1	0.24	0.89	0.39	
AT1G18570	MYB51	0.99	1.68	0.22	X

Osmotic Stress and Hormonal Cross Talk in the Growing Leaves

As hormonal cross talk plays an essential role for both growth and environmental responses, transcriptome data were compared with available hormone addition experiments (Goda et al., 2008). This comparison revealed that ethylene-responsive genes were enriched among the transcripts affected in P and E leaves (Supplemental Table S3). Osmotic stress significantly enhanced the expression of genes encoding ethylene signaling components, such as ethylene re-

ceptors (ESR1 and ESR2) and ethylene response factors (ERF2, ERF4, and ERF5; Fig. 7A; Supplemental Table S2). Consistent with the expression data, the growth of ethylene-insensitive mutants was more sensitive to 25 mM mannitol, and mutants developed severe phenotypes characterized by growth arrest and curled, pale leaves. As anticipated, the *ein2.5* plants, for which the ethylene insensitivity was the strongest, also responded most clearly to the mannitol treatment (Fig. 7, B and C). Moreover, we found a possible involvement of gibberellin (GA) signaling in growth

Figure 6. Increased starch levels in mannitol-grown plants. A, MapMan representation of starch metabolism. Red and blue, Down-regulated and up-regulated genes, respectively; E25-E0 and M25-M0, E and M leaves (25–0 mM), respectively. B, Lugol's staining of 15-DAS plants harvested 8 h into the day. Note intense blue staining of the mannitol-grown seedling.



adaptation, as predicted targets of the DELLA transcription factors were very significantly enriched in the P and E samples (Table I; Supplemental Table S3). In contrast, auxin-responsive genes were specifically down-regulated in E leaves (e.g. *SHY1*, *SHY2*, *BDL*, and *PIN1*); accordingly, the response of P and E leaves shared a significant similarity with the transcriptional response to chemical treatments employing auxin inhibitors (2,3,5-triiodobenzoic acid and 2,4,6-trichlorophenoxyacetic acid; Fig. 7A; Supplemental Table S3).

Cell Wall Metabolism Is Affected in the E Leaves

To explain the reduced growth of mannitol-treated seedlings, genes involved in cell division and cell expansion are among the prime suspects. Osmotic stress resulted in the differential expression of many cell wall-related genes, of which the majority were in the E leaves (Fig. 8A; Supplemental Table S2). Overall, genes related to cell wall synthesis (cell wall precursors and cellulose synthesis) and those encoding arabinogalactan proteins were down-regulated, while genes involved in conferring cell wall extensibility (xyloglucan transferases and expansins) and cell wall degradation were evenly distributed among up- and down-regulated transcripts. Interestingly, expression was induced for three pectin methyl esterase genes that can mediate changes in cell wall pH. Additionally, considering the proposed role of superoxide in affecting cell wall extensibility, we utilized nitroblue tetrazolium (NBT) staining to investigate superoxide accumulation in the growing and M leaves. This analysis revealed that superoxide levels increased exclusively in mannitol-grown E leaves (Fig. 8B), while no accumulation could be detected in P or M leaves. No significant differences were found in transcripts of either the core cell cycle (Vandepoele et al., 2002) or associated with cell division (Menges et al., 2003), consistent with identical cell proliferation rates at the time P samples were taken.

Alternative Respiration Is of Key Importance for Cell Division

Of the interesting transcripts induced by mannitol exclusively in the P leaves was the gene encoding an alternative oxidase (*AOX1a*) that plays a major role in the alternative respiratory pathway in Arabidopsis mitochondria (Giraud et al., 2008, 2009; Ho et al., 2008). *AOX1a* was strongly coexpressed with a number of genes referred to as “mitochondrial dysfunction regulon” (Van Aken et al., 2007), containing other mitochondrial genes (mitochondrial small heat shock protein *HSP23.5*, AAA-type ATPase *BCS1*, NADH dehydrogenase *NDB4*, and unknown proteins targeted to the mitochondria), MATE transporters, glutathione S-transferases, transcription factors, cytochrome P450, and steroid sulfotransferase. Sixteen out of these 25 genes were also up-regulated by mannitol, of which 13 responded only in the P leaves (Fig. 9A). To confirm these changes and to provide further spatial resolution, promoter:GUS reporter lines were constructed for eight of the 13 overlapping mitochondrial dysfunction regulon genes (see “Materials and Methods”). The obtained GUS staining agreed very well with the microarray data, confirming induction for seven out of eight genes in the P or P and E leaves (Fig. 9, A and B; Supplemental Fig. S8). At the spatial level, GUS induction was not just observed in fully P leaves but also in leaves that were partially P (i.e. that had already started to differentiate at their tip; Fig. 9B; Supplemental Fig. S8). Moreover, this analysis allowed the response of other leaves to be studied. Induction was not restricted to leaf 3 but could be observed in young leaves throughout plant development. To investigate whether changes in the expression of genes from the mitochondrial dysfunction regulon translated into a cellular phenotype, mitochondria of SAM and P leaves were examined by transmission electron microscopy (Fig. 9, C and D). A significant difference in the SAM sections of the mannitol-grown seedlings

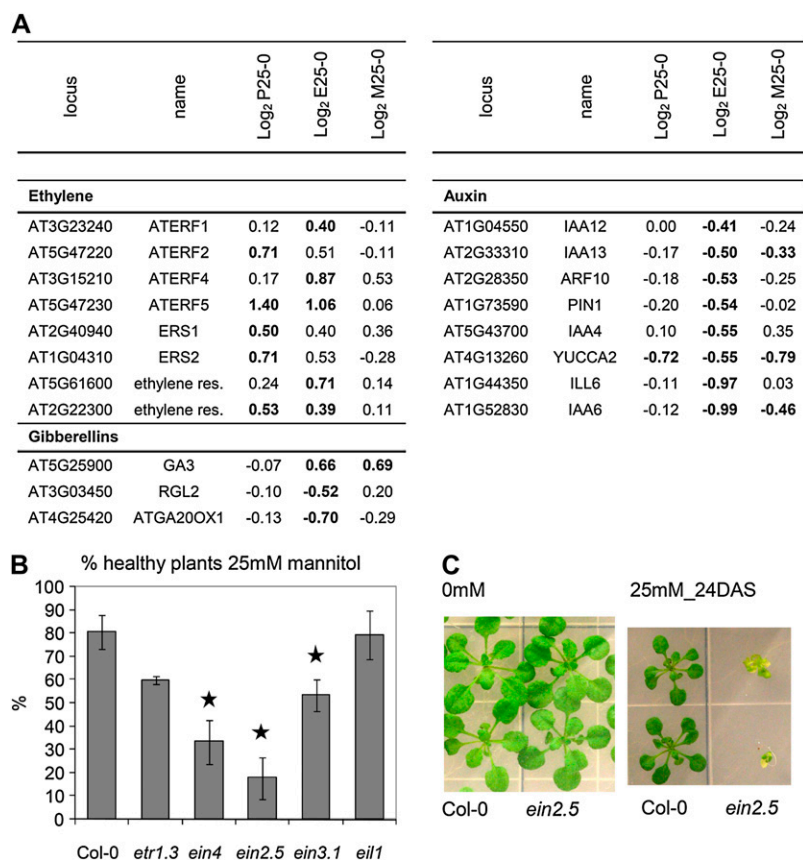


Figure 7. Importance of ethylene signaling for stress tolerance of growing leaves. A, Expression changes for the selected genes involved in ethylene, GA, and auxin signaling and metabolism. Boldface indicates significance (global test; $P < 0.05$). B, Analysis of ethylene-insensitive mutants. Plants that developed a severe phenotype (curled pale leaves, growth arrest) were scored and used to calculate percentage of the “healthy”-looking seedlings. Stars indicate significance (t test; $P < 0.05$). Data are means \pm SE of multiple plates. C, Wild-type and *ein2.5* plants grown on medium without or with 25 mM mannitol. [See online article for color version of this figure.]

was the presence of large mitochondria. In addition, in both SAM and leaf sections, mitochondria were rounder, which could be expressed as increased circularity index.

The proposed role of AOX is to prevent overreduction of the mitochondrial electron transport chain (mETC) under stress conditions and, therefore, the formation of ROS. Accordingly, superoxide levels were comparable in control and stressed P leaves visualized with NBT staining (Fig. 8B). Another proposed role of alternative respiration is to enable ATP

production directly from the glycolysis and to support growth under conditions in which the mETC is inhibited, such as drought stress. To determine whether AOX plays a role in growth adaptation, the growth of *AOX1a*-overexpressing plants (*AOX-OE*) was measured with or without mannitol. Leaf areas were recorded daily between 9 and 23 DAS, and the obtained data were used to calculate the percentage of reduction of leaf area caused by stress. Early on and under optimal conditions, the leaf area of *AOX-OE* plants was reduced by approximately 20%, but it

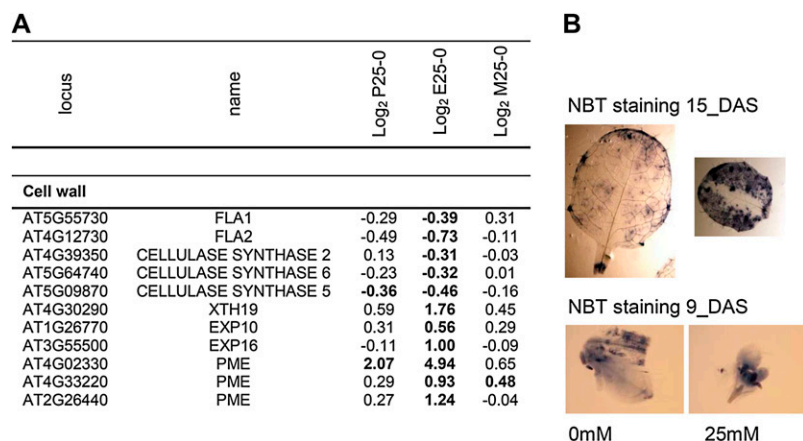


Figure 8. Cell wall-related genes and superoxide levels affected by osmotic stress in the E leaves. A, Expression changes for the selected genes involved in cell wall metabolism. Boldface indicates significance (global test; $P < 0.05$). B, Superoxide levels visualized in leaf 3 from 9- and 15-DAS plants grown without (left) or with (right) mannitol stained with NBT. [See online article for color version of this figure.]

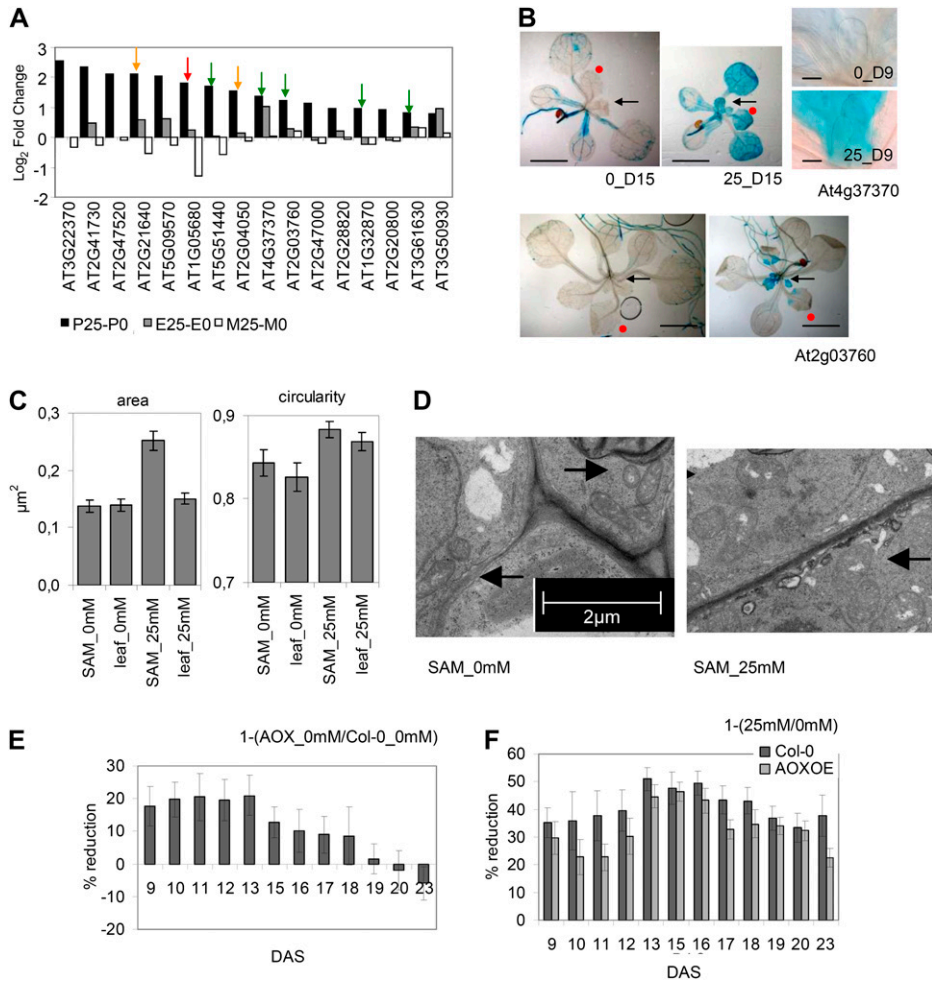


Figure 9. Importance of alternative respiration in P leaves. A, Log₂ fold change of genes from the mitochondrial dysfunction regulon in long-term mannitol experiments measured in P, E, and M leaves. Arrows indicate genes used for promoter:GUS analysis; green, orange, and red arrows indicate expression validated by GUS staining, in one of two GUS lines, and not validated, respectively. B, Photographs of 15-DAS plants of two promoter:GUS lines. The arrows mark young, P leaves (note induction of both genes). The red dots indicate the third E leaf (note induction of *At4g37370* gene only). Photographs of the third leaf from the 9-DAS *At4g37370*:GUS line showed a strong induction. C, Transmission electron micrographs of control and mannitol-grown plants (P leaf 3 and SAM) were used to calculate area and circularity of the mitochondria. Data are means ± SE of 40 to 60 mitochondria. D, Transmission electron micrographs of SAM from control and mannitol-grown seedlings. Arrows point to mitochondria clusters. E and F, Leaf area measured for leaf 3 dissected from control (Col-0) and *AOX1a-OE* plants grown without or with 25 mM mannitol from 9 DAS until 22 DAS. Obtained data were used to calculate percentage reduction under control conditions (*AOX-OE*, 0 mM; Col-0, 0 mM; E) and stress conditions (25 mM/0 mM; F). Data are means ± SE of eight to 10 leaves.

caught up with control plants by 19 DAS (Fig. 9E). At the same time, the leaf area measured for plants grown on mannitol was the same or even larger for *AOX-OE* plants, which translated into a lower percentage of reduction, on average by approximately 7% to 8% (Fig. 9F). To investigate whether the enhanced growth of *AOX-OE* plants under osmotic stress would translate into better performance under drought, an in soil drought assay was developed. Water-saturated soil was used to germinate seeds, allowed to dry until it reached a relative water content (RWC) of 68% (control conditions), 60% (mild drought), or 55% (severe

drought), and afterward RWC was kept constant (Fig. 10A). Similar to the in vitro *AOX-OE* plants, plants were smaller under normal conditions, but we measured no differences in daily changes in soil water status between wild-type and *AOX-OE* plants (Fig. 10B). Importantly, relative growth rates of wild-type and *AOX-OE* plants measured under control conditions were not significantly different, indicating that the observed size reduction arose during early seedling establishment. Mild and severe drought resulted in decreased growth rates; as a consequence, the final size of the wild-type rosettes was reduced by 16% and

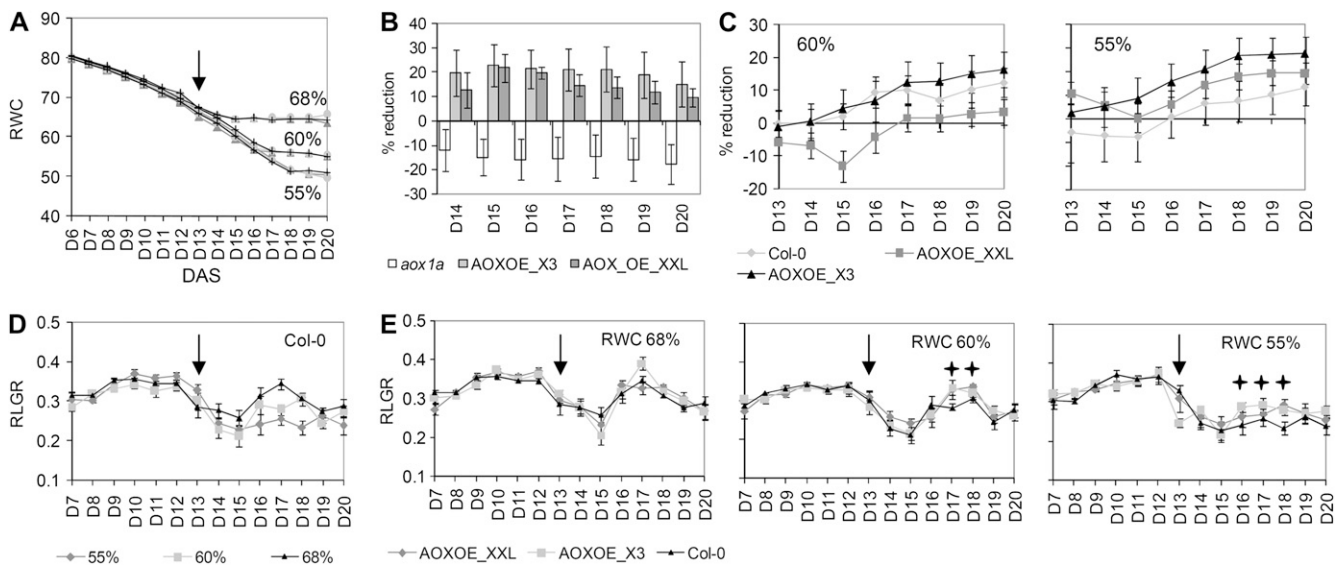


Figure 10. Less reduced growth of the *AOX-OE* plants during soil drought. A, RWC determined throughout the experiment (6–20 DAS) based on pot weight taken before watering. Stress treatment started at 13 DAS (arrow) when control plants were first watered to RWC of 68%. Black and gray lines, Col-0 and *AOX-OE* plants, respectively. B, Percentage reduction of *AOX-OE* and *aox1a* rosette area compared with wild-type (Col-0) plants measured under control conditions (RWC 68%). C, Percentage reduction of Col-0 and *AOX-OE* rosette area under mild (RWC 60%) and severe (RWC 55%) drought compared with control conditions from 13 to 20 DAS (duration of stress treatment). D, Relative growth rates (RLGR) of Col-0 under control and drought conditions. Note reduction of RLGR associated with stress onset (arrow). E, RLGR of Col-0 and *AOX-OE* plants under control and drought conditions. Arrows indicate start of stress treatment. Note the less reduced RLGR measured for *AOX-OE* plants (crosses). Data are means \pm se from eight to 10 plants for each genotype and treatment. *AOXOE_X3* and *AOXOE_XXL* are two independent *AOX1a*-overexpressing lines, while *aox1a* stands for the *AOX1a* knockout mutant.

27% (at 20 DAS), respectively (Fig. 10, C and D). Like osmotic stress, this reduction was lower for the two independent *AOX-OE* lines due to higher growth rates (Fig. 10, C and E). In addition to overexpressors, also *aox1a* knockout plants were included in the experiment. These plants were 15% larger under normal conditions but had no growth phenotype under drought stress (Fig. 10B), possibly due to the redundancy with other *AOX* genes. In conclusion, our data indicate that changes in mitochondrial metabolism support cell proliferation under stress conditions.

DISCUSSION

Phenotypic Plasticity of Arabidopsis Leaves to Water-Limiting Conditions

Phenotypic plasticity allows a plant to manage its resources under changing environmental conditions. Reduction of the final leaf size is an important adaptive response to many abiotic and biotic stresses. Stable soil water deficits affect both the final cell number and the size of Arabidopsis leaves; however, it is still unclear how these changes arise (Aguirrezabal et al., 2006). Here, we provide insight into the kinetics of leaf growth under steady and relatively mild osmotic stress that, similar to drought, reduces both cell num-

ber and size. Reduction of cell number was shown to occur during very early leaf development. From approximately 4 d after leaf initiation (9 DAS) onward, cell division rates were indistinguishable or even slightly higher in stressed plants than in control plants. It is plausible that stress affects the duration of the first few divisions in the emerging leaves and/or fewer cells are recruited from the meristem into the leaf primordia. The latter would imply regulation of the leaf size at the SAM level, which, to our knowledge, has not been described previously. On the contrary, the SAM size has previously been associated with number rather than with size of initiated leaves (Clark et al., 1993; Mauseth, 2004; Boucheron et al., 2005). Similar to cell number, cell size was also reduced by stress early in leaf development, with expansion rates that were lower during the first few days after cell differentiation and became indistinguishable or higher in stressed versus control plants from 15 DAS onward. These higher cell division and expansion rates measured late during the proliferation and expansion stages, respectively, marginally compensated the initial reduction in cell number and size. This observation is in agreement with previous studies demonstrating compensation occurring in Arabidopsis leaves subjected to drought (Aguirrezabal et al., 2006; Pereyra-Irujo et al., 2008). Stress not only affected final leaf size but also the SI, resulting in decreased stomatal density, which can be interpreted as an adaptation to minimize water loss.

Similar observations had been made previously for birch (*Betula pendula*; Pääkkönen et al., 1998) and senna (*Cassia angustifolia*; Ratnayaka and Kincaid, 2005). While the number of stomata decreased, trichome density increased. Trichomes are known to positively affect the water economy in leaves, primarily through the increased reflection of solar radiation and reduction of leaf temperature and, hence, transpiration rate. Accordingly, trichome density has proved to be an important adaptive trait to drought stress (Gianoli and González-Teuber, 2005). It would be interesting to investigate how mild drought stress affects the signaling networks involved in stomata and trichome development. In conclusion, leaf growth rate can very well adapt to stress conditions, and the initial reduction of cell proliferation and cell expansion can be considered as an important adaptive response to generate smaller organs. Importantly, the obtained growth data provided a basis for sample selection for further profiling analysis. As growth rates of stressed and control plants were identical at the time of sampling, growth adaptation rather than growth repression was clearly under investigation.

Response of Arabidopsis Leaves to Osmotic Stress Depends on the Developmental Stage

Developmental input into the stress response of growing and M leaves is the major contribution of this work and allowed the identification of candidate processes involved in growth adaptation to stress. Although it could be anticipated that the response to osmotic stress would differ between leaves at different developmental stages, the extent of these differences was greater than expected. Only 20 genes, mainly general stress markers such as *CYP79B2* and *chitinase* (*At2g43570*), were up-regulated by osmotic stress at all three leaf stages, while hundreds of transcripts and a number of metabolites changed exclusively at one leaf stage. Importantly, osmotic stress response of P and E leaves shared high overlap, pointing to common mechanisms that allow growth adaptation to stress in addition to stage-specific processes. A much smaller, but significant, overlap was also measured between stress response of E and M leaves, both at the transcript and metabolite levels, most probably illustrating their photosynthetic status. Virtually no overlap was detected between P and M leaves. Additionally, the obtained results strongly argue that by zooming in on selected developmental stages, a serious dilution of information is avoided and that even a relatively mild stress results in hundreds of transcript and multiple metabolite changes that would not be identified using whole-seedling data. Finally, our work demonstrated that young Arabidopsis seedlings are most similar to the E leaves. In conclusion, similar to the transcriptional responses to high salinity of specific root cell types (Dinneny et al., 2008), this work argues for the importance of spatial and developmental resolution to

fully understand different aspects of stress tolerance of multicellular organisms.

Classical Stress Response Dominates in M Leaves

Published profiling experiments, performed mainly on M leaves (Bouchabke-Coussa et al., 2008; Giraud et al., 2008; Perera et al., 2008; Zhang et al., 2008) or complete plant shoots (Seki et al., 2002; Catala et al., 2007; Kilian et al., 2007; Matsui et al., 2008; Weston et al., 2008; Zeller et al., 2009) and under relatively severe drought or osmotic conditions (Seki et al., 2002; Catala et al., 2007; Matsui et al., 2008; Urano et al., 2009), have led to the identification of a set of transcriptional and metabolic responses associated with drought stress. Also in our experiments, M leaves showed the classical drought stress response, validating the treatment (for an overview, see Fig. 11), but the response was much less pronounced in E leaves and only marginal in P leaves. Accumulation of LEA proteins, Pro, and flavonoids in the M leaves could be related to their role in protecting the photosynthetic and enzymatic machinery of source leaves against oxidative damage that would be less important in E, but particularly in P, leaves (Havaux and Kloppstech, 2001; Mowla et al., 2006; Verslues et al., 2006, and refs. within). Accordingly, diaminobenzidine and NBT staining revealed no differences in either hydrogen peroxide or superoxide levels in M leaves or in the operating efficiency of PSII. In fact, both starch and reducing sugars (Glc and Fru) accumulated in both E

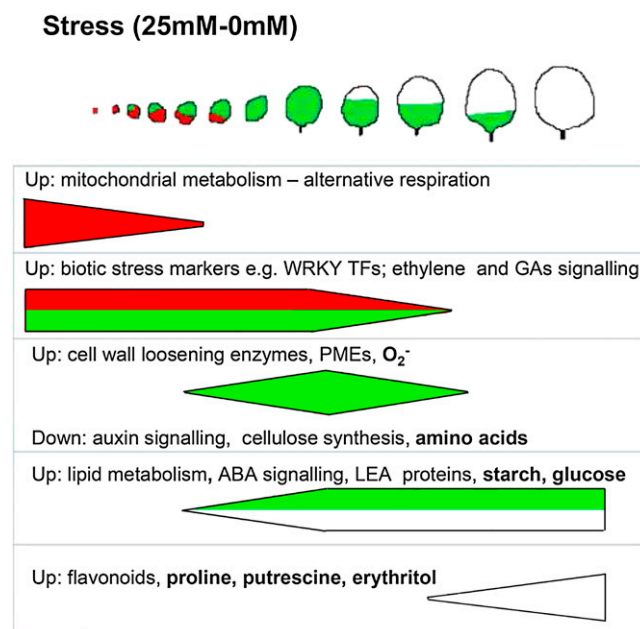


Figure 11. Schematic representation of processes, genes, and metabolites (boldface) affected by stress (25–0 mM). PMEs, Pectin methyl esterases; TFs, transcription factors. Dark gray (red online), light gray (green online), and white represent P, E, and M cells, respectively. [See online article for color version of this figure.]

and M leaves, indicating carbon abundance. Glc could contribute to a decrease in cell water potential and has been observed to increase in Arabidopsis and in grapevine (*Vitis vinifera*) subjected to long-term drought (Rizhsky et al., 2004; Cramer et al., 2007). The role of starch is less clear and is possibly the indirect effect of Glc accumulation. In addition, production of waxes and cuticle thickening, as circumstantially suggested by the microarray data, would further prevent water loss from the leaf surface (Samuels et al., 2008). In conclusion, M and, to a lesser extent, E leaves tolerate osmotic stress by exploiting classical drought responses, validating the osmotic stress assay as a good proxy for drought stress.

DELLA and Ethylene Cross Talk in Growth Regulation of P and E Leaves

Only a few genes and metabolites have been shown to be involved in the regulation of leaf growth under adverse environmental conditions (Granier and Tardieu, 2009). Among these, a prominent role belongs to the DELLA transcription factors. Different abiotic and biotic stresses affect GA levels, stabilizing DELLA, which in turn restrict plant growth and activate tolerance mechanisms, possibly by modulating ROS metabolism (Achard et al., 2006, 2008; Navarro et al., 2008). Microarray analysis revealed a clear involvement of DELLA and ethylene-responsive genes in the adaptation of the P and E leaf tissues to mild osmotic stress. Ethylene, which accumulates under stress, has importantly been shown to cross talk with DELLA factors, promoting their stabilization in both GA-dependent and -independent manners (for review, see Yoo et al., 2009). Thus, ethylene and GA seemingly play a major role in regulating both cell proliferation and expansion under stress conditions, whereas ABA is mainly important in the M tissues. Further support of this finding was provided by the proposal that ethylene is a primary drought signal for growing leaves while ABA is a primary drought signal for the M leaves of tomato (*Solanum lycopersicum*; Sobeih et al., 2004). The importance of ethylene signaling could be further validated with ethylene-insensitive mutants that were much more sensitive to mild osmotic stress. The strength of the phenotype corresponded very well with the degree of ethylene insensitivity. While *ein2.5* plants were characterized by almost complete growth arrest, the performance of the weak ethylene-insensitive mutant *eil1* was comparable with that of wild-type plants. Activation of the ethylene signaling could also explain the up-regulation of at least a proportion of genes classically associated with biotic stress measured in the growing leaves, and these will be interesting targets to study their role in osmotic stress tolerance. Extensive overlap between abiotic and biotic signaling has been reported previously, so it is not surprising that genes classically associated with biotic stresses could also play an important role under abiotic conditions (Narusaka et al., 2004;

Kankainen et al., 2006; for review, see Fujita et al., 2006; Walley et al., 2007). Good examples are the disease resistance regulator *OCP3*, *PR-3*, and *GmERF3*, recently shown to confer tolerance not only to biotic but also to abiotic agents, including drought, salt, and osmotic stress (Seo et al., 2008; Ramírez et al., 2009; Zhang et al., 2009). In summary, although ABA, ethylene, and DELLA proteins have been implicated in stress tolerance previously, the temporal context shows that they are developmentally separated. Additionally, our work presents a number of candidate genes classically associated with biotic stress, such as WRKY (*WRKY53*, *WRKY15*, and *WRKY33*) and ERF (*ERF5* and *ERF2*) transcription factors, to test their function in stress tolerance and growth adaptation to osmotic stress. Interestingly, *WRKY15* and *WRKY33* were also among the DELLA target genes (Navarro et al., 2008).

Cell Wall Loosening Drives Cell Expansion at the Lower Turgor Pressure

Water loss changes turgor pressure and, thus, directly affects cell expansion. Previous work, done primarily on maize (*Zea mays*) roots, has demonstrated that cell wall loosening facilitates growth at low turgor pressures. Abundance and activity of cell wall-loosening enzymes (expansins and xyloglucan endotransglucosylase/hydrolases [XTHs]), pH, ROS accumulation, and cellulose production have been proposed to be involved in the increasing cell wall extensibility (Wu and Cosgrove, 2000; Sharp et al., 2004; Zhu et al., 2007; Moore et al., 2008). We provide evidence for similar mechanisms acting in E leaves of Arabidopsis subjected to osmotic stress. Superoxide levels were exclusively elevated in the E leaves, consistent with earlier findings showing that the generation of hydroxyl radicals from superoxide and hydrogen peroxide plays a direct role in cell wall loosening via polysaccharide cleavage under both favorable and drought stress conditions (Liszakay et al., 2003; Zhu et al., 2007). The expression of a number of genes involved in the regulation of cell wall extensibility was up-regulated (for review, see Moore et al., 2008), encoding expansins and XTHs including *EXP10* and *XTH19* (Cho and Cosgrove, 2000; Vissenberg et al., 2005; Osato et al., 2006). Wall-loosening activity of expansins has been linked to acidic growth (Cosgrove, 2000), and microarray data revealed up-regulation of three genes encoding pectin methyl esterase (*AT4G02330*, *AT2G26440*, and *AT4G33220*) that can reduce the cell wall pH by converting methoxyl groups of pectins to carboxyl groups accompanied by proton release (Wen et al., 1999). Finally, expression of cellulose synthesis genes was reduced, which might result in further cell wall weakening. Decrease of cellulose content was observed in tobacco (*Nicotiana tabacum*) cell cultures treated with high concentration of PEG, which had been proposed to divert carbon from cell walls into compatible solute synthesis, contributing to the osmotic adjustment (Iraki et al., 1989). In conclusion, these data emphasize the

importance of the cell wall for growth adaptation of Arabidopsis leaves subjected to long-term osmotic stress and identify a number of candidate genes involved in cell wall loosening, such as XTH19 and three pectin methyl esterases.

Alternative Respiration Is Essential in the P Leaves

The mitochondrial dysfunction regulon comprises 25 genes that are tightly coexpressed under a number of stress treatments that affect the mitochondrial electron transport chain and up-regulated in the transgenic lines overexpressing mitochondria-associated prohibitin genes (Van Aken et al., 2007). Although the exact role of the mitochondrial dysfunction regulon is still a subject of debate, proteins encoded by the regulon are probably involved in the maintenance of mitochondrial function and morphology. One of the regulon genes encodes an alternative oxidase that shortcuts the mETC by transferring electrons directly to oxygen, providing plants with an alternative electron transport pathway. As alternative respiration limits oxidative phosphorylation and ATP production, it is mainly employed under stress conditions that negatively affect components of the mETC and ATP synthase complex, thereby preventing ROS formation (Sweetlove et al., 2002; Umbach et al., 2005; Rhoads et al., 2006; Giraud et al., 2008; Ho et al., 2008). Moreover, together with cytosolic or mitochondrial NADH dehydrogenase, AOX provides a path to recycle cytosolic NAD⁺-supporting glycolysis and ATP synthesis, via substrate phosphorylation, or to recycle NAD⁺ required for the tricarboxylic acid cycle and, hence, nucleotide and amino acid synthesis, respectively (for review, see Fernie et al., 2004). As energy, nucleotides, and amino acids are indispensable for cell division and ROS can cause serious damage to replicating DNA, alternative respiration would certainly be of central importance for growth maintenance in the P leaves. In accordance, expression of *AOX1a*, *NDB4*, and other genes of the mitochondrial dysfunction regulon was induced in the P, but not the E or M, leaves. Moreover, larger and rounder mitochondria found in the actively P cells of the SAM provide further evidence to link the mitochondrial dysfunction regulon with the maintenance of cell division rates under stress conditions. Promoter:GUS lines confirmed the induction of genes of the mitochondrial dysfunction regulon in young P and differentiating leaves throughout plant growth. As anticipated, growth of *AOX-OE* plants was less reduced by mild osmotic stress very early during leaf development, indicating that cell proliferation was responsible for the observed phenotype. Importantly, better growth performance was also measured under controlled drought treatment in soil, providing evidence that osmotic stress can be used as a good proxy for drought. Importantly, we measured no differences in daily changes in soil water status between wild-type and *AOX-OE* plants, indicating that all plants experi-

enced the same control and stress conditions, so the observed growth improvement could not be solely attributed to smaller *AOX-OE* rosette size. Smaller and larger rosettes of *AOX-OE* and *aox1a* plants, respectively, further indicate that mETC is a preferable energy source under favorable conditions and alternative oxidation under stress conditions. Interestingly, enhanced growth was also observed for *AOX-OE* under cold, although the cellular basis of this finding was not investigated (Fiorani et al., 2005), and the *aox1a* mutant was much more sensitive to combined drought and light stress (Giraud et al., 2008). In conclusion, profiling data followed by targeted analysis of the transgenic plants proved that alternative respiration supports cell proliferation under stress conditions. Importantly, these results also indicate a prominent role for the other mitochondrial dysfunction regulon genes that will be further studied in relation to growth and stress regulation.

CONCLUSION

This study demonstrates that, rather than being a secondary effect of compromised photosynthesis and carbon limitation, reduction of leaf growth is an important adaptive response to osmotic stress. Molecular profiling of actively growing and M leaves offered developmental resolution to stress responses, allowing the distinction of biological processes important for M and/or growing leaves. By zooming in on selected developmental stages, a serious dilution of information was avoided, revealing new insights and demonstrating that many changes measured in whole plants are in fact developmentally separated. The obtained data indicate that both cell proliferation and expansion are regulated by common regulatory cascades involving ethylene and GAs but not ABA signaling, while downstream effector genes are stage specific. Among these are enzymes supporting cell expansion under low turgor pressure and mitochondrial genes crucial for maintaining cell proliferation. To validate profiling data, the latter were confirmed with transgenic lines overexpressing the *AOX1a* gene in both osmotic and drought stress assays. Notably, data mining identified candidate genes that would be interesting in relation to growth and stress regulation, such as those from the mitochondrial dysfunction regulon and those encoding WRKY and ERF transcription factors. In summary, this work significantly contributes to the understanding of growth and stress physiology by providing a developmental input into stress responses and demonstrating the importance of mitochondrial metabolism in the P leaves.

MATERIALS AND METHODS

Plant Growth

Seedlings of Arabidopsis (*Arabidopsis thaliana* ecotype Columbia-0 [Col-0]) were grown in vitro in half-strength Murashige and Skoog (1962) medium

supplemented with 1% Suc under a 16-h-day ($110 \mu\text{mol m}^{-2} \text{s}^{-1}$) and 8-h-night regime. Before autoclaving, 25 mM mannitol (Sigma) was added to the agar medium, while PEG-infused plates were prepared according to van der Weele et al. (2000) with 10 mM overlay of PEG 3500 (Sigma).

Growth Analysis

Leaf 3 was harvested daily from 9 to 22 DAS from eight to 10 plants in three independent experiments. After clearing with 70% ethanol, leaves were mounted in lactic acid on microscope slides. Epidermal cells (40–100 cells) were drawn for four leaves with a DMLB microscope (Leica) fitted with a drawing tubus and a differential interference contrast objective, while leaves were photographed under a binocular. Photographs of leaves and drawings were used to measure the leaf area and the cell size, respectively, with the ImageJ software. Leaf area and cell size were subsequently used to calculate cell numbers. The SI is the percentage of stomatas per all cells. Means of leaf area, cell size, and cell number were transformed logarithmically and locally fitted to a quadratic function of which the first derivative was taken as the relative growth rate (De Veylder et al., 2001). Mean values of the three biological experiments were used for statistical analysis.

Drought Assay

Water deficit was imposed by controlling and stabilizing the soil water status during the development of soil-grown plants. Plants were germinated in cylindrical polypropylene pots (200 mL, diameter 53 mm, height 88 mm; VWR International) with side cuts for faster desiccation and filled with water-saturated soil. The soil was allowed to dry until it reached RWCs of 68%, 60%, and 55% and subsequently watered daily to maintain a constant water status based on the pot weight. RWC was defined as the ratio of percentage water to dry soil, which in this case was always 30 ± 0.5 g (RWC = mass of water/mass of water + mass of dry soil). Photographs were taken daily and used to extract total rosette areas, from which relative growth rates were subsequently calculated ($[\ln \text{ rosette area day } 2 - \ln \text{ rosette area day } 1]/\text{time}$). Plants were grown under 110 to 120 $\mu\text{mol m}^{-2} \text{s}^{-1}$ light and an 8-h-night regime. A detailed description of the drought assays will be published elsewhere.

Sampling for Profiling Analysis

Leaf 3 was harvested from plants at 9, 15, and 22 DAS, while seedlings reached stage 1.03 (third leaf, 1 mm in size) around 11 DAS. All samples were from three independent experiments and from multiple plates within the experiment. Complete harvest was done in growth chambers starting at 2 h into the day and took less than 15 min. As leaf initiation and developmental timing were not affected, samples were harvested simultaneously from both control and mannitol-treated plants. Because of their small size, leaves from plants at 9 DAS were dissected under a binocular microscope. Briefly, whole seedlings were harvested in an excess of RNAlater solution (Ambion) and, after overnight in 4°C, dissected on the cooling plate using the binocular microscope with precision microscissors. Dissected leaves were transferred to a new tube, frozen in liquid nitrogen, and ground with a Retsch machine and 3-mm metal balls. Microarray analysis, qRT-PCR confirmation, and metabolite measurements were carried out on material harvested from separate experiments.

RNA Extraction

RNA was extracted with Trizol according to the manufacturer's protocol (Invitrogen) and 4 μg of glycogen as carrier during the precipitation step. RNA samples were subjected to DNA digestion (Roche) and subsequently to the RNeasy clean-up kit (Qiagen).

ATH1 Expression Profiling and Data Analysis

RNA samples (three biological replicates for each treatment and stage) were hybridized to single Affymetrix ATH1 genome arrays at the Flanders Institute for Biotechnology Microarray Facility in Leuven, Belgium. Expression data were processed with Robust Multichip Average background correction, normalization, summarization, and BioConductor (Irizarry et al., 2003a, 2003b; Gentleman et al., 2004). An alternative cdf (tinesath1cdf) was used, in which each probe is uniquely assigned to one transcript (Casneuf

et al., 2007; <http://www.bioconductor.org/packages/release/data/experiment/html/tinesath1cdf.html>). BioConductor package Limma was used to identify differentially expressed genes (Smyth, 2004). A factorial design (mannitol treatment 25–0 mM and developmental stage P-E-M) was applied to analyze the data. For comparisons of interest, moderated *t* statistics with the eBayes method were used, and *P* values were corrected for multiple testing (for each contrast separately using topTable; Hochberg and Benjamini, 1990). In addition, we applied a more stringent correction for multiple testing across genes and across contrasts with decideTest (global; Supplemental Tables S1 and S2). Importantly, lists of significant genes obtained with both methods were very similar, leading to identical conclusions. Besides the moderated *t* statistics for each pairwise contrast, we calculated global *F* statistics to identify the genes that were affected in at least one contrast (Supplemental Tables S1 and S2). Two-fold changes in expression (only for 0–0 mM comparisons) and decideTest (global) cutoffs of less than 0.05 were used to delineate gene lists of interest. Further subsets of these differentially expressed gene lists were identified and subjected to overrepresentation analysis.

Comparison with Publicly Available Microarray Data

Selected public microarray data were grouped according to experiment type (e.g. abiotic stress and hormone treatment; Supplemental Table S3). Groups of experiments were Robust Multichip Average processed and subjected to Limma analysis, as described above. Sets of responsive genes were delineated always with a 2-fold expression change and false discovery rate-corrected *P* value cutoffs of less than 0.05. Although these cutoffs were chosen somewhat arbitrarily, we assessed the robustness of the results by testing more and less stringent cutoffs. All tests gave very similar results (data not shown). The lists of responsive genes were compared with those identified in our microarray experiment to identify global trends in the functional repertoire of the affected genes that were used as hints to explore the results in more detail. Overrepresentation was tested by means of Fisher exact tests followed by Bonferroni *P* value correction.

Metabolite Analysis

Metabolite data were obtained from nine samples harvested from three independent experiments. The relative levels of metabolites were determined with an established gas chromatography-time-of-flight-mass spectrometry protocol exactly as described by Lisek et al. (2006). Chromatograms and mass spectra were evaluated by Chroma TOF 1.6 (Leco) and TagFinder 4.0 (Luedemann et al., 2008). The amount of metabolites was analyzed as relative metabolite abundance calculated by normalization of the signal intensity to that of [¹³C]sorbitol, which was added as an internal standard, and fresh weight.

qRT-PCR

For cDNA synthesis, 100 ng to 2 μg of RNA was used with the SuperScript Reverse III reagent (Invitrogen) according to the manufacturer's instructions. Primers were designed with the QuantPrime (Arvidsson et al., 2008) Web site (Supplemental Table S5). qRT-PCR was done on a LightCycler 480 (Roche Diagnostics) on 384-well plates with LightCycler 480 SYBR Green I Master (Roche) according to the manufacturer's recommendations. Melting curves were analyzed to check primer specificity. Normalization was done against the average of housekeeping genes *UBQ10*, *GAPDH*, and *CBP20*: $\Delta\text{Ct} = \text{Ct}(\text{gene}) - \text{Ct}(\text{mean}[\text{housekeeping genes}])$ and $\Delta\Delta\text{Ct} = \Delta\text{Ct}(\text{control}) - \Delta\text{Ct}(\text{mannitol or PEG})$. ΔCt values for the three biological replicates were used for statistical analysis. Ct refers to the number of cycles at which SYBR Green fluorescence reaches an arbitrary value during the exponential phase of the cDNA amplification.

Lugol's, NBT, and GUS Staining

Multiple plants at 15 and 22 DAS were cleared in 70% ethanol, stained for 20 min with an excess of Lugol's solution (Sigma), and subsequently washed with water. Multiple leaves from three independent experiments were stained for 1 h with 0.1% NBT (Sigma) solution in complete darkness and, subsequently, cleared in 80% boiling ethanol.

Whole plantlets were harvested after 9, 15, and 22 d and incubated in 90% acetone (4°C) for 30 min, washed in 100 mM Tris-HCl/50 mM NaCl (pH 7.0), and subsequently incubated in 5-bromo-4-chloro-3-indolyl- β -glucuronide

(X-gluc) buffer (100 mM Tris-HCl/50 mM NaCl buffer [pH 7.0], 2 mM $K_3[Fe(CN)_6]$, and 4 mM X-gluc) at 37°C for 2.5 h. Seedlings were washed in 100 mM Tris-HCl/50 mM NaCl (pH 7.0) and cleared overnight in 90% lactic acid. Samples were photographed under a differential interference contrast microscope (Leica).

Transmission Electron Microscopy

Young leaves and SAM of 9-DAS seedlings were excised, immersed in a fixative solution of 2% paraformaldehyde and 2.5% glutaraldehyde, and postfixed in 1% OsO_4 with 1.5% $K_3Fe(CN)_6$ in 0.1 M Na-cacodylate buffer (pH 7.2) for 1 h under vacuum infiltration at room temperature and 4 h of rotation at room temperature, followed by overnight fixation at 4°C. After washing three times for 20 min with the buffer, samples were dehydrated through a graded ethanol series, including a bulk staining with 2% uranyl acetate at the 50% ethanol step, followed by embedding in Spurr's resin. Ultrathin sections of a gold interference color were cut with an ultramicrotome (Leica EM UC6), poststained with uranyl acetate and lead citrate (Leica EM AC20), collected on formvar-coated copper slot grids, and viewed with a transmission electron microscope (1010; JEOL).

Transgenic Lines and Mutants

Seeds of *AOX-OE* lines were kindly provided by Prof. James E. Siedow (Duke University; Fiorani et al., 2005). *CYCB1;2:DB-GUS* lines were a kind gift of Dr. Peter Doerner (University of Edinburgh). For generation of *promoter:GFP-GUS* lines, genomic DNA was isolated from Arabidopsis (Col-0) with DNeasy plant kits (Qiagen) according to the manufacturer's instructions. The 1,500-bp genomic regions (or the intergenic region in the case of nearby coding sequences) upstream of the specific start codon were amplified by PCR with the Platinum Taq High Fidelity DNA polymerase (Invitrogen) and the forward and reverse primers (Supplemental Table S5). The PCR products were cloned into pDONR221 and cloned by recombination to pBGWFS7, generating a transcriptional GFP-GUS fusion. The constructs were transformed into Arabidopsis Col-0 by *Agrobacterium tumefaciens*-mediated floral dipping. Transformants with the *bar* resistance gene were selected by spraying with 40 mg L⁻¹ Pestanal (glufosinate ammonium; Sigma-Aldrich). Transformants with a single insertion locus, and subsequently homozygous lines, were selected by segregation analysis on Murashige and Skoog medium containing 5 mg L⁻¹ glufosinate ammonium. All analyses were performed with non-segregating homozygous T3 transgenic lines. Ethylene-insensitive and *aox1a* mutants were obtained from the Arabidopsis Seed Stock Center (*ein2.5* [N8844], *ein3.1* [N8052], *eil1* [655070], *etr1.3* [N3070], *ein4* [N8053], and *aox1a* [N584897]).

Operating Efficiency of PSII

Operating efficiency of PSII was measured using the IMAGING-PAM Chlorophyll Fluorometer (Heinz Walz) in three independent experiments.

Microarray data from this article were deposited in the Gene Expression Omnibus database (GSE16474).

Supplemental Data

The following materials are available in the online version of this article.

Supplemental Figure S1. Variable phenotypes of PEG-grown plants.

Supplemental Figure S2. Percentage reduction of cell number, size, and SI measured for leaf 3 dissected from plants grown without or with 25 mM mannitol.

Supplemental Figure S3. Leaf ploidy is not affected by mannitol.

Supplemental Figure S4. Cellular analysis of PEG-grown plants.

Supplemental Figure S5. Classification of transcripts differentially expressed during leaf development (0–0 mm).

Supplemental Figure S6. Validation of microarray data by qRT-PCR.

Supplemental Figure S7. Overlap between osmotic stress and leaf profiling data.

Supplemental Figure S8. Validation of microarray data with promoter:GUS lines of the genes from the mitochondrial dysfunction regulon.

Supplemental Table S1. Genes differentially regulated during development.

Supplemental Table S2. Expression data for the mannitol treatment.

Supplemental Table S3. Comparison with publicly available expression data sets.

Supplemental Table S4. Gas chromatography-mass spectrometry metabolite data.

Supplemental Table S5. List of primers used in qRT-PCR experiments and cloning of promoter:GUS lines.

ACKNOWLEDGMENTS

We thank Dr. Nathalie Gonzalez, Dr. Korneel Vandenbroucke, and Prof. Gerrit Beemster for useful discussion, Katrien Maleux for technical assistance, Bjorn De Meyer and Stijn Dhondt for help in establishing the drought assay, and Dr. Martine De Cock for help in preparing the manuscript.

Received October 7, 2009; accepted November 6, 2009; published November 11, 2009.

LITERATURE CITED

- Achard P, Cheng H, De Grauwe L, Decat J, Schoutteten H, Moritz T, Van Der Straeten D, Peng J, Harberd NP (2006) Integration of plant responses to environmentally activated phytohormonal signals. *Science* **311**: 91–94
- Achard P, Renou J-P, Berthomé R, Harberd NP, Genschik P (2008) Plant DELLAs restrain growth and promote survival of adversity by reducing the levels of reactive oxygen species. *Curr Biol* **18**: 656–660
- Aguirrezabal L, Bouchier-Combaud S, Radziejowski A, Dautat M, Cookson SJ, Granier C (2006) Plasticity to soil water deficit in *Arabidopsis thaliana*: dissection of leaf development into underlying growth dynamic and cellular variables reveals invisible phenotypes. *Plant Cell Environ* **29**: 2216–2227
- Arvidsson S, Kwasniewski M, Riaño-Pachón DM, Mueller-Roeber B (2008) QuantPrime—a flexible tool for reliable high-throughput primer design for quantitative PCR. *BMC Bioinformatics* **9**: 465
- Beemster GTS, De Veylder L, Vercruyse S, West G, Rombaut D, Van Hummelen P, Galichet A, Gruissem W, Inzé D, Vuylsteke M (2005) Genome-wide analysis of gene expression profiles associated with cell cycle transitions in growing organs of Arabidopsis. *Plant Physiol* **138**: 734–743
- Bouchabke-Coussa O, Quashie M-L, Seoane-Redondo J, Fortabat M-N, Gery C, Yu A, Linderme D, Trouverie J, Granier F, Téoulé E, et al (2008) *ESKIMO1* is a key gene involved in water economy as well as cold acclimation and salt tolerance. *BMC Plant Biol* **8**: 125
- Boucheron E, Healy JHS, Bajon C, Sauvanet A, Rembur J, Noin M, Sekine M, Riou Khamlichi C, Murray JAH, Van Onckelen H, et al (2005) Ectopic expression of *Arabidopsis* *CYCD2* and *CYCD3* in tobacco has distinct effects on the structural organization of the shoot apical meristem. *J Exp Bot* **56**: 123–134
- Boyer JS (1982) Plant productivity and environment. *Science* **218**: 443–448
- Boyes DC, Zayed AM, Ascenzi R, McCaskill AJ, Hoffman NE, Davis KR, Görlach J (2001) Growth stage-based phenotypic analysis of *Arabidopsis*: a model for high throughput functional genomics in plants. *Plant Cell* **13**: 1499–1510
- Bursens S, Himanen K, van de Cotte B, Beekman T, Van Montagu M, Inzé D, Verbruggen N (2000) Expression of cell cycle regulatory genes and morphological alterations in response to salt stress in *Arabidopsis thaliana*. *Planta* **211**: 632–640
- Casneuf T, Van de Peer Y, Huber W (2007) In situ analysis of cross-hybridisation on microarrays and the inference of expression correlation. *BMC Bioinformatics* **8**: 461
- Catala R, Ouyang J, Abreu IA, Hu Y, Seo H, Zhang X, Chua N-H (2007)

- The *Arabidopsis* E3 SUMO ligase SIZ1 regulates plant growth and drought responses. *Plant Cell* **19**: 2952–2966
- Cho H-T, Cosgrove DJ** (2000) Altered expression of expansin modulates leaf growth and pedicel abscission in *Arabidopsis thaliana*. *Proc Natl Acad Sci USA* **97**: 9783–9788
- Clark SE, Running MP, Meyerowitz EM** (1993) *CLAVATA1*, a regulator of meristem and flower development in *Arabidopsis*. *Development* **119**: 397–418
- Cosgrove DJ** (2000) Loosening of plant cell walls by expansins. *Nature* **407**: 321–326
- Cramer GR, Ergül A, Grimplet J, Tattersall EAR, Bohlman MC, Vincent D, Sonderegger J, Evans J, Osborne C, et al** (2007) Water and salinity stress in grapevines: early and late changes in transcript and metabolite profiles. *Funct Integr Genomics* **7**: 111–134
- De Veylder L, Beeckman T, Beeckman GTS, Krols L, Terras F, Landrieu I, Van Der Schueren E, Maes S, Naudts M, Inzé D** (2001) Functional analysis of cyclin-dependent kinase inhibitors of *Arabidopsis*. *Plant Cell* **13**: 1653–1667
- Dinneny JR, Long TA, Wang JY, Jung JW, Mace D, Pointer S, Barron C, Brady SM, Schiefelbein J, Benfey PN** (2008) Cell identity mediates the response of *Arabidopsis* roots to abiotic stress. *Science* **320**: 942–945
- Donnelly PM, Bonetta D, Tsukaya H, Dengler RE, Dengler NG** (1999) Cell cycling and cell enlargement in developing leaves of *Arabidopsis*. *Dev Biol* **215**: 407–419
- Fernie AR, Carrari F, Sweetlove LJ** (2004) Respiratory metabolism: glycolysis, the TCA cycle and mitochondrial electron transport. *Curr Opin Plant Biol* **7**: 254–261
- Fiorani F, Umbach AL, Siedow JN** (2005) The alternative oxidase of plant mitochondria is involved in the acclimation of shoot growth at low temperature: a study of *Arabidopsis AOX1a* transgenic plants. *Plant Physiol* **139**: 1795–1805
- Fricke W, Akhiyarova G, Wei W, Alexandersson E, Miller A, Kjellbom PO, Richardson A, Wojciechowski T, Schreiber L, Veselov D, et al** (2006) The short-term growth response to salt of the developing barley leaf. *J Exp Bot* **57**: 1079–1095
- Fujita M, Fujita Y, Noutoshi Y, Takahashi F, Narusaka Y, Yamaguchi-Shinozaki K, Shinozaki K** (2006) Crosstalk between abiotic and biotic stress responses: a current view from the points of convergence in the stress signaling networks. *Curr Opin Plant Biol* **9**: 436–442
- Gentleman RC, Carey VJ, Bates DM, Bolstad B, Dettling M, Dudoit S, Ellis B, Gautier L, Ge Y, Gentry J, et al** (2004) Bioconductor: open software development for computational biology and bioinformatics. *Genome Biol* **5**: R80
- Gianoli E, González-Teuber M** (2005) Environmental heterogeneity and population differentiation in plasticity to drought in *Convolvulus chilensis* (Convolvulaceae). *Evol Ecol* **19**: 603–613
- Giraud E, Ho LHM, Clifton R, Carroll A, Estavillo G, Tan YF, Howell KA, Ivanova A, Pogson B, Millar AH, et al** (2008) The absence of ALTER-NATIVE OXIDASE1a in *Arabidopsis* results in acute sensitivity to combined light and drought stress. *Plant Physiol* **147**: 595–610
- Giraud E, Van Aken O, Ho LHM, Whelan J** (2009) The transcription factor ABI4 is a regulator of mitochondrial retrograde expression of *ALTER-NATIVE OXIDASE1a*. *Plant Physiol* **150**: 1286–1296
- Godá H, Sasaki E, Akiyama K, Maruyama-Nakashita A, Nakabayashi K, Li W, Ogawa M, Yamauchi Y, Preston J, Aoki K, et al** (2008) The AtGenExpress hormone and chemical treatment data set: experimental design, data evaluation, model data analysis and data access. *Plant J* **55**: 526–542
- Granier C, Tardieu F** (2009) Multi-scale phenotyping of leaf expansion in response to environmental changes: the whole is more than the sum of parts. *Plant Cell Environ* **32**: 1175–1184
- Havaux M, Kloppstech K** (2001) The protective functions of carotenoid and flavonoid pigments against excess visible radiation at chilling temperature investigated in *Arabidopsis npq* and *tt* mutants. *Planta* **213**: 953–966
- Ho LHM, Giraud E, Uggalla V, Lister R, Clifton R, Glen A, Thirkettle-Watts D, Van Aken O, Whelan J** (2008) Identification of regulatory pathways controlling gene expression of stress-responsive mitochondrial proteins in *Arabidopsis*. *Plant Physiol* **147**: 1858–1873
- Hochberg Y, Benjamini Y** (1990) More powerful procedures for multiple significance testing. *Stat Med* **9**: 811–818
- Hsiao TC, Xu L-K** (2000) Sensitivity of growth of roots versus leaves to water stress: biophysical analysis and relation to water transport. *J Exp Bot* **51**: 1595–1616
- Inzé D, De Veylder L** (2006) Cell cycle regulation in plant development. *Annu Rev Genet* **40**: 77–105
- Iraki NM, Singh N, Bressan RA, Carpita NC** (1989) Cell walls of tobacco cells and changes in composition associated with reduced growth upon adaptation to water and saline stress. *Plant Physiol* **91**: 48–53
- Irizarry RA, Bolstad BM, Collin F, Cope LM, Hobbs B, Speed TP** (2003a) Summaries of Affymetrix GeneChip probe level data. *Nucleic Acids Res* **31**: e15
- Irizarry RA, Hobbs B, Collin F, Beazer-Barclay YD, Antonellis KJ, Scherf U, Speed TP** (2003b) Exploration, normalization, and summaries of high density oligonucleotide array probe level data. *Biostatistics* **4**: 249–264
- Kankainen M, Brader G, Törönen P, Palva ET, Holm L** (2006) Identifying functional gene sets from hierarchically clustered expression data: map of abiotic stress regulated genes in *Arabidopsis thaliana*. *Nucleic Acids Res* **34**: e124
- Kilian J, Whitehead D, Horak J, Wanke D, Weinl S, Batistic O, D'Angelo C, Bornberg-Bauer E, Kudla J, Harter K** (2007) The AtGenExpress global stress expression data set: protocols, evaluation and model data analysis of UV-B light, drought and cold stress responses. *Plant J* **50**: 347–363
- Lisec J, Schauer N, Kopka J, Willmitzer L, Fernie AR** (2006) Gas chromatography mass spectrometry-based metabolite profiling in plants. *Nat Protoc* **1**: 387–396
- Liszak A, Kenk B, Schopfer P** (2003) Evidence for the involvement of cell wall peroxidase in the generation of hydroxyl radicals mediating extension growth. *Planta* **217**: 658–667
- Luedemann A, Strassburg K, Erban A, Kopka J** (2008) TagFinder for the quantitative analysis of gas chromatography-mass spectrometry (GC-MS)-based metabolite profiling experiments. *Bioinformatics* **24**: 732–737
- Matsui A, Ishida J, Morosawa T, Mochizuki Y, Kaminuma E, Endo TA, Okamoto M, Nambara E, Nakajima M, Kawashima M, et al** (2008) *Arabidopsis* transcriptome analysis under drought, cold, high-salinity and ABA treatment conditions using a tiling array. *Plant Cell Physiol* **49**: 1135–1149
- Mauseth JD** (2004) Giant shoot apical meristems in cacti have ordinary leaf primordia but altered phyllotaxy and shoot diameter. *Ann Bot (Lond)* **94**: 145–153
- Menges M, Hennig L, Gruissem W, Murray JAH** (2003) Genome-wide gene expression in an *Arabidopsis* cell suspension. *Plant Mol Biol* **53**: 423–442
- Moore JP, Vitré-Gibouin M, Farrant JM, Driouich A** (2008) Adaptations of higher plant cell walls to water loss: drought vs desiccation. *Physiol Plant* **134**: 237–245
- Mowla SB, Cuyper A, Driscoll SP, Kiddle G, Thomson J, Foyer CH, Theodoulou FL** (2006) Yeast complementation reveals a role for an *Arabidopsis thaliana* late embryogenesis abundant (LEA)-like protein in oxidative stress tolerance. *Plant J* **48**: 743–756
- Murashige T, Skoog F** (1962) A revised medium for rapid growth and bioassays with tobacco tissue cultures. *Physiol Plant* **15**: 473–497
- Narusaka M, Narusaka Y, Seki M, Ishida J, Nakashima M, Enju A, Sakurai T, Satou M, Shinozaki K** (2004) Crosstalk in the responses to biotic and abiotic stresses in *Arabidopsis*. *Plant Cell Physiol (Suppl)* **45**: S188
- Navarro L, Bari R, Achard P, Lisón P, Nemri A, Harberd NP, Jones JDG** (2008) DELLAs control plant immune responses by modulating the balance of jasmonic acid and salicylic acid signaling. *Curr Biol* **18**: 650–655
- Osato Y, Yokoyama R, Nishitani K** (2006) A principal role for AtXTH18 in *Arabidopsis thaliana* root growth: a functional analysis using RNAi plants. *J Plant Res* **119**: 153–162
- Pääkkönen E, Vahala J, Pohjola M, Holopainen T, Kärenlampi L** (1998) Physiological, stomatal and ultrastructural ozone responses in birch (*Betula pendula* Roth.) are modified by water stress. *Plant Cell Environ* **21**: 671–684
- Perera IY, Hung C-Y, Moore CD, Stevenson-Paulik J, Boss WF** (2008) Transgenic *Arabidopsis* plants expressing the type 1 inositol 5-phosphatase exhibit increased drought tolerance and altered abscisic acid signaling. *Plant Cell* **20**: 2876–2893
- Pereyra-Irujo GA, Velázquez L, Lechner L, Aguirrezábal LAN** (2008) Genetic variability for leaf growth rate and duration under water deficit in sunflower: analysis of responses at cell, organ, and plant level. *J Exp Bot* **59**: 2221–2232
- Ramírez V, Coego A, López A, Agorio A, Flors V, Vera P** (2009) Drought

- tolerance in Arabidopsis is controlled by the *OCP3* disease resistance regulator. *Plant J* **58**: 578–591
- Ratnayaka HH, Kincaid D** (2005) Gas exchange and leaf ultrastructure of tinnevely senna, *Cassia angustifolia*, under drought and nitrogen stress. *Crop Sci* **45**: 840–847
- Rhoads DM, Umbach AL, Subbaiah CC, Siedow JN** (2006) Mitochondrial reactive oxygen species: contribution to oxidative stress and interorganellar signaling. *Plant Physiol* **141**: 357–366
- Rizhsky L, Liang H, Shuman J, Shulaev V, Davletova S, Mittler R** (2004) When defense pathways collide: the response of Arabidopsis to a combination of drought and heat stress. *Plant Physiol* **134**: 1683–1696
- Samuels L, Kunst L, Jetter R** (2008) Sealing plant surfaces: cuticular wax formation by epidermal cells. *Annu Rev Plant Biol* **59**: 683–707
- Seki M, Narusaka M, Junko I, Nanjo T, Fujita M, Youko O, Kamiya A, Nakajima M, Enju A, Dakurai T, et al** (2002) Monitoring the expression profiles of 7000 Arabidopsis genes under drought, cold and high salinity stresses using a full-length cDNA microarray. *Plant J* **31**: 279–292
- Seki M, Umezawa T, Urano K, Shinozaki K** (2007) Regulatory metabolic networks in drought stress responses. *Curr Opin Plant Biol* **10**: 296–302
- Seo PJ, Lee AK, Xiang F, Park CM** (2008) Molecular and functional profiling of *Arabidopsis pathogenesis-related* genes: insights into their roles in salt response of seed germination. *Plant Cell Physiol* **49**: 334–344
- Sharp RE, Poroyko V, Hejlek LG, Spollen WG, Springer GK, Bohnert HJ, Nguyen HT** (2004) Root growth maintenance during water deficits: physiology to functional genomics. *J Exp Bot* **55**: 2343–2351
- Smyth GK** (2004) Linear models and empirical Bayes methods for assessing differential expression in microarray experiments. *Stat Appl Genet Mol Biol* **3**: Article 3
- Sobeih WY, Dodd IC, Bacon MA, Grierson D, Davies WJ** (2004) Long-distance signals regulating stomatal conductance and leaf growth in tomato (*Lycopersicon esculentum*) plants subjected to partial root-zone drying. *J Exp Bot* **55**: 2353–2363
- Sweetlove LJ, Heazlewood JL, Herald V, Holtzapffel R, Day DA, Leaver CJ, Millar AH** (2002) The impact of oxidative stress on *Arabidopsis* mitochondria. *Plant J* **32**: 891–904
- Thimm O, Bläsing O, Gibon Y, Nagel A, Meyer S, Krüger P, Selbig J, Müller LA, Rhee SY, Stitt M** (2004) MAPMAN: a user-driven tool to display genomics data sets onto diagrams of metabolic pathways and other biological processes. *Plant J* **37**: 914–939
- Umbach AL, Fiorani F, Siedow JN** (2005) Characterization of transformed Arabidopsis with altered alternative oxidase levels and analysis of effects on reactive oxygen species in tissue. *Plant Physiol* **139**: 1806–1820
- Urano K, Maruyama K, Ogata Y, Morishita Y, Takeda M, Sakurai N, Suzuki H, Saito K, Shibata D, Kobayashi M, et al** (2009) Characterization of the ABA-regulated global responses to dehydration in Arabidopsis by metabolomics. *Plant J* **57**: 1065–1078
- Usadel B, Nagel A, Steinhäuser D, Gibon Y, Bläsing OE, Redestig H, Sreenivasulu N, Krall L, Hannah MA, Poree F, et al** (2006) PageMan: an interactive ontology tool to generate, display, and annotate overview graphs for profiling experiments. *BMC Bioinformatics* **7**: 535
- Van Aken O, Pečenková T, van de Cotte B, De Rycke R, Eeckhout D, Fromm H, De Jaeger G, Witters E, Beemster GTS, Inzé D, et al** (2007) Mitochondrial type-I prohibitins of *Arabidopsis thaliana* are required for supporting proficient meristem development. *Plant J* **52**: 850–864
- Vandepoel K, Raes J, De Veylder L, Rouzé P, Rombauts S, Inzé D** (2002) Genome-wide analysis of core cell cycle genes in *Arabidopsis*. *Plant Cell* **14**: 903–916
- van der Weele CM, Spollen WG, Sharp RE, Baskin TI** (2000) Growth of *Arabidopsis thaliana* seedlings under water deficit studied by control of water potential in nutrient-agar media. *J Exp Bot* **51**: 1555–1562
- Verslues PE, Agarwal M, Katiyar-Agarwal S, Zhu J, Zhu J-K** (2006) Methods and concepts in quantifying resistance to drought, salt and freezing, abiotic stresses that affect plant water status. *Plant J* **45**: 523–539
- Veselov DS, Mustafina AR, Sabirjanova IB, Akhilarova GR, Dedov AV, Veselov SU, Kudoyarova GR** (2002) Effect of PEG-treatment on the leaf growth response and auxin content in shoots of wheat seedlings. *Plant Growth Regul* **38**: 191–194
- Vissenberg K, Oyama M, Osato Y, Yokoyama R, Verbelen J-P, Nishitani K** (2005) Differential expression of *AtXTH17*, *AtXTH19* and *AtXTH20* genes in *Arabidopsis* roots: physiological roles in specification in cell wall construction. *Plant Cell Physiol* **46**: 192–200
- Walley JW, Coughlan S, Hudson ME, Covington ME, Kaspi R, Banu G, Harmer SL, Dehesh K** (2007) Mechanical stress induces biotic and abiotic stress responses via a novel *cis*-element. *PLoS Genet* **3**: e172
- Wen F, Zhu Y, Hawes MC** (1999) Effect of pectin methylesterase gene expression on pea root development. *Plant Cell* **11**: 1129–1140
- West G, Inzé D, Beemster GTS** (2004) Cell cycle modulation in the response of the primary root of Arabidopsis to salt stress. *Plant Physiol* **135**: 1050–1058
- Weston DJ, Gunter LE, Rogers A, Wullschlegel SD** (2008) Connecting genes, coexpression modules, and molecular signatures to environmental stress phenotypes in plants. *BMC Syst Biol* **2**: 16
- Wu Y, Cosgrove DJ** (2000) Adaptation of roots to low water potentials by changes in cell wall extensibility and cell wall proteins. *J Exp Bot* **51**: 1543–1553
- Yoo S-D, Cho Y, Sheen J** (2009) Emerging connections in the ethylene signaling network. *Trends Plant Sci* **14**: 270–279
- Zeller G, Henz SR, Widmer CK, Sachsenberg T, Rättsch G, Weigel D, Laubinger S** (2009) Stress-induced changes in the *Arabidopsis thaliana* transcriptome analyzed using whole-genome tiling arrays. *Plant J* **58**: 1068–1082
- Zhang G, Chen M, Li L, Xu Z, Chen X, Guo J, Ma Y** (2009) Overexpression of the soybean *GmERF3* gene, an AP2/ERF type transcription factor for increased tolerances to salt, drought, and diseases in transgenic tobacco. *J Exp Bot* **60**: 3781–3796
- Zhang Y, Xu W, Li Z, Deng XW, Wu W, Xue Y** (2008) F-box protein DOR functions as a novel inhibitory factor for abscisic acid-induced stomatal closure under drought stress in Arabidopsis. *Plant Physiol* **148**: 2121–2133
- Zhu J, Alvarez S, Marsh EL, LeNoble ME, Cho I-J, Sivaguru M, Chen S, Nguyen HT, Wu Y, Schachtman DP, et al** (2007) Cell wall proteome in the maize primary root elongation zone. II. Region-specific changes in water soluble and lightly ionically bound proteins under water deficit. *Plant Physiol* **145**: 1533–1548